Induction of Positive Cellular and Humoral Immune Responses by a Prime-Boost Vaccine Encoded with Simian Immunodeficiency Virus *gag/pol*[1]

Kenji Someya,* Yasushi Ami,† Tadashi Nakasone,* Yasuyuki Izumi,* Kazuhiro Matsuo,* Shigeo Horibata,* Ke-Qin Xin,‡ Hiroshi Yamamoto,§ Kenji Okuda,‡ Naoki Yamamoto,* and Mitsuo Honda[2]*

It is believed likely that immune responses are responsible for controlling viral load and infection. In this study, when macaques were primed with plasmid DNA encoding SIV *gag* and *pol* genes (SIV*gag/pol* DNA) and then boosted with replication-deficient vaccinia virus DIs recombinant expressing the same genes (rDIsSIV*gag/pol*), this prime-boost regimen generated higher levels of Gag-specific CD4$^+$ and CD8$^+$ T cell responses than did either SIV*gag/pol* DNA or rDIsSIV*gag/pol* alone. When the macaques were i.v. challenged with pathogenic simian/HIV, the prime-boost group maintained high CD4$^+$ T cell counts and reduced plasma viral loads up to 30 wk after viral challenge, whereas the rDIsSIV*gag/pol* group showed only a partial attenuation of the viral infection, and the group immunized with SIV*gag/pol* DNA alone showed none at all. The protection levels were better correlated with the levels of virus-specific T cell responses than the levels of neutralization Ab responses. These results demonstrate that a vaccine regimen that primes with DNA and then boosts with a replication-defective vaccinia virus DIs generates anti-SIV immunity, suggesting that it will be a promising vaccine regimen for HIV-1 vaccine development. *The Journal of Immunology,* **2006, 176: 1784–1795.**

The primary goals of any prophylactic HIV vaccine are to induce HIV-specific immune responses capable of preventing the malfunctioning of immune systems and to limit viral transmission due to replication. Clinical studies have demonstrated that CTL immune responses are associated with the reduction of plasma viral load (1, 2) and can control disease progression (3, 4). Replication of pathogenic SIV in vivo has also been shown to be controlled in the macaque model by CD8$^+$ T cell responses (5). Because amino acid sequences of Gag and Pol of HIV-1 proteins are relatively conserved, cross-clade and broad CTL responses targeting those proteins have been observed in both HIV-infected and HIV-exposed individuals, even if the latter group had not become infected (6–8). Thus, one recent focus of HIV vaccine research has been to elicit more protective antiviral immune responses by enhancing the expression levels of HIV-1 Ags of Gag and Pol using a safe vaccine vector.

Recently, several prime-boost regimens consisting of a DNA prime and a recombinant poxvirus boost targeting the immunodeficiency virus have been reported to generate higher levels of HIV-specific T cell immune responses than regimens relying on DNA or recombinant poxvirus vaccine alone (9, 10). In efficacy trials of such heterologous prime-boost vaccines, an SIV Ag encoding DNA prime and a boost of recombinant modified vaccinia virus Ankara (MVA)[3] elicited effective anti-SIV immunity and controlled infection of the nonpathogenic simian-HIV (SHIV) strain as well as of the pathogenic strain SHIV-89.6P in macaques (11–13) by effectively inducing CD8$^+$ CTL immunities. Various poxvirus vectors, i.e., an avipox virus, a canarypox virus, a fowlpox virus, a substrain of vaccinia Copenhagen (NYVAC), and MVA, have been evaluated for their usefulness, either alone or in combination with other vaccine modalities (14–18). To be useful, these vaccine vectors must, of course, be safe. The currently widely used MVA, which was developed toward the end of the campaign to eradicate small pox, has been effectively and safely used in >100,000 people as a small pox vaccine (19). MVA-based recombinant vector has also been reported to be safe in animals (20, 21). Lately, we have developed a replication-defective vaccinia virus DIs strain as a vaccine vector (22, 23). The DIs strain, generated by a 1-day-old egg passage of the DIE strain (24), has been proven safe (25, 26). We also suggested that a new prime-boost vaccine regimen consisting of SIV*gag/pol* DNA and rDIsSIV*gag/pol* might be useful for the development of an HIV-1 candidate vaccine that could induce strong cellular protective responses in mice (23). Lately, similar DNA/MVA vaccine combinations support the idea that the vaccine induced strong Ag-specific T and B cell responses (27). The prime-boost-vaccinated mice generated higher levels of both Gag-specific CD4$^+$ and CD8$^+$ T cell immune responses than those vaccinated with either DNA or rDIs alone. When such mice were challenged with SIV *gag/pol* expressing

*AIDS Research Center, National Institute of Infectious Diseases, Tokyo, Japan; †Division of Experimental Animal Research, National Institute of Infectious Diseases, Tokyo, Japan; ‡Department of Bacteriology, Yokohama City University, School of Medicine, Yokohama, Japan; and §Laboratory Animal Research Center, Toyama Medical and Pharmaceutical University, Toyama, Japan

Received for publication June 28, 2005. Accepted for publication November 4, 2005.

The costs of publication of this article were defrayed in part by the payment of page charges. This article must therefore be hereby marked *advertisement* in accordance with 18 U.S.C. Section 1734 solely to indicate this fact.

[1] This work was supported by the Panel on AIDS of the U.S.-Japan Cooperative Medical Science Program; the Human Science Foundation, Japan; the Japanese Ministry of Health, Labor, and Welfare; and the AIDS Vaccine Project in conjunction with the Japan Science and Technology Corporation.

[2] Address correspondence and reprint requests to Dr. Mitsuo Honda, AIDS Research Center, National Institute of Infectious Diseases, 1-23-1 Toyama, Shinjuku-ku, Tokyo 162-8640, Japan. E-mail address: mhonda@nih.go.jp

[3] Abbreviations used in this paper: MVA, modified vaccinia virus Ankara; rDIsSIV*gag/pol*, recombinant DIs expressing SIV*gag* and *pol*; SFC, spot-forming cell; SHIV, simian-human immunodeficiency virus; SIV*gag/pol* DNA, plasmid DNA encoding SIV *gag* and *pol* genes; $TCID_{50}$, 50% tissue culture infectious doses.

0022-1767/06/$02.00

wild-type recombinant vaccinia virus, viral replication in the ovaries was controlled even in the absence of anti-DIs immunity. These results suggest that the new vaccine regimen, consisting of a DNA prime and a vaccinia virus DIs boost, safely and effectively elicits anti-immunodeficiency viral immunity.

In this study, we evaluated the vaccine efficacy of the prime-boost DNA/DIs vaccine encoding the *gag/pol* gene against a challenge with a highly pathogenic SHIV using 19 macaques. We hypothesize that the efficacy is mediated not only by the effect of virus-specific cellular immunity, but also by the effect of neutralization Ab responses against the challenged virus.

Materials and Methods

Animals

Nineteen female adult cynomolgus macaques (*Macaca fascicularis*) were purchased from Japan SLC. The macaques were fed and cared for in accordance with the standard operating procedure approved by the Ministry of Education, Culture, Sports, Science, and Technology of Japan. The study was performed in the P3 facility under guidelines established by the laboratory biosafety manual of the World Health Organization (28).

Preparation of vaccine Ags and challenge virus

Plasmid DNA encoding SIV *gag* and *pol* genes (SIV*gag/pol* DNA) and recombinant DIs expressing the same genes (rDIsSIV*gag/pol*) were prepared as previously described (22, 23, 29). pcDNA3.1$^-$ and rDIsLacZ were used as controls of plasmid and recombinant viral Ags, respectively. After being immunized according to the protocol, animals were challenged with SHIV-C2/1 (30–32), which was a SHIV-89.6 variant isolated at the peak of initial plasma viremia from an infected cynomolgus macaque (31). The original SHIV strain was provided by Dr. Y. Lu (Harvard AIDS Institute, Cambridge, MA) (33, 34).

Enumeration of T PBL

Fifty microliters of whole heparinized blood samples were stained with anti-human CD3 (clone HIT3a; BD Pharmingen), anti-human CD4 (clone SK3; BD Biosciences), and anti-human CD8 (clone SK1; BD Biosciences) for 15 min at 4°C. Blood samples were treated with FACS lysing solution for 15 min at 4°C, and then 50 μl of Flow Count (Beckman Coulter) was added. A FACSCalibur flow cytometer (BD Biosciences) was used to acquire 5000 CD3-positive, lymphocyte-gated events.

Intracellular IFN-γ cytokine staining

Approximately 10^6 of fresh PBMC were incubated with 0.2 μM pooled SIV Gag peptides spanning the full length of the Gag protein (AIDS Research and Reference Program, National Institutes of Health) together with 1 μg of anti-human CD28 (clone KOLT-2; Nichirei) and 1 μg of anti-human CD49d (clone 9F10; BD Pharmingen) in an appropriate volume of RPMI 1640 supplemented with 10% FBS and antibiotics for 16 h at 37°C. Then brefeldin A (Sigma-Aldrich) was added at 10 μg/ml, and the cells were incubated for an additional 4 h. After incubation, the cells were washed, stained with anti-human CD3 (clone HIT3a; BD Pharmingen) and anti-human CD8 (clone SK1; BD Biosciences) or anti-human CD4 (clone SK3; BD Biosciences) for 15 min. The cells were washed and then treated sequentially with FACS-lysing solution (BD Biosciences) and permeablizing solution (BD Biosciences) for 10 min. The cells were stained with anti-human IFN-γ-FITC (clone 45.15; Immuno Tech) for 30 min and fixed with 2% paraformaldehyde solution. A FACSCalibur flow cytometer (BD Biosciences) was used to acquire 20,000 lymphocyte-gated events, which were then analyzed with CellQuest software (BD Biosciences).

Virus-specific IFN-γ ELISPOT assay

An ELISPOT assay was performed following the method developed by Mothe and Watkins of the Wisconsin University Primate Center (35). Ninety-six-well, flat-bottom plates were coated with anti-IFN-γ mAb (clone MD-1; U-CyTech-BV) and blocked with 2% BSA in PBS. Fresh PBMC were added to the plate at 2×10^5 cells/well in triplicate and then incubated with 0.2 μM pooled SIV Gag peptides (AIDS Research and Reference Program) for 16 h at 37°C. Gold-labeled anti-biotin IgG solution (U-CyTech-BV) was added to the washed plates, which were then incubated for 1 h at 37°C. Individual spot-forming cells (SFC) were counted using the KS ELISPOT compact system (Zeiss) after a 15-min reaction with an activator mix (U-CyTech-BV). An SFC was defined as a large black spot with a fuzzy border (34).

Abs to SIV Gag p27 and SHIV 89.6P Env

SIV Gag- and SHIV Env-specific IgG Ab end-point titers of the macaques' sera were measured by ELISA as previously described (23, 27, 30). All samples were run in triplicate at several dilutions. In brief, 96-well ELISA plates were coated with 0.3 μg of SIV p27 Gag (Advanced Biotechnologies) or 0.2 μM pooled SHIV 89.6P Env peptides (AIDS Research and Reference Program) per well. Heat-inactivated sera were serially diluted, then added to the ELISA plates. Gag- and Env-specific Abs bound to the Ags were captured with alkaline phosphatase-labeled goat anti-mouse IgG (EY Laboratories) and *p*-nitrophenyl-phosphate disodium substrate (Invitrogen Life Technologies).

The SHIV Env-specific neutralization Ab responses induced by challenge with SHIV were analyzed as previously described (28). In brief, 10 μg/ml purified macaque IgG was incubated with 100 50% tissue culture infectious doses ($TCID_{50}$) of SHIV-C2/1, then cultured in M8166 cells. The result was compared with parallel cultures to which preimmune IgG had been added. Neutralization was expressed as the percent inhibition of SIV Gag production in the culture supernatants. Anything >20% of inhibition was considered to be an efficient neutralization response.

Quantitation of plasma viral load

Quantitation of SHIV genomic RNA copies in plasma samples was performed by real-time PCR with a TaqMan assay kit (PerkinElmer Applied Biosystems) and a PRISM 7700 sequence detection system (PerkinElmer Applied Biosystems) as previously described (30). Genomic RNA extracted from plasma samples and SIVmac239 (RNA standard; 5.4×10^4 RNA copies) were subjected to RT-PCR using an SIVmac239–1224 forward, SIVmac239–1326 reverse primer pair and an FAM-SIV-1272T probe. RNA copy numbers from plasma samples were calculated from the standard curve. Data were expressed as RNA copies per milliliter of plasma.

Flow cytometric detection of various subpopulations in CD4$^+$ T cells

Approximately 10^6 fresh PBMC were stained with anti-human CD4 (clone SK3; BD Biosciences), anti-human CD29 (clone 4B4; Beckman Coulter), and anti-human CD45RA (clone 5H9; BD Pharmingen) or with anti-human CD4 (clone ν-TH/I; Nichirei) and anti-human CD28 (clone KOLT-2, Nichirei). A FACSCalibur (BD Biosciences) was used to acquire 10,000 lymphocyte-gated events, which were then analyzed with CellQuest software.

Statistical analysis

Data are expressed as the mean $\pm$ SD. The data analysis was conducted using the StatView program (SAS Institute), and all reported p values are two-sided. Comparisons between groups were performed using the Kruskal-Wallis H test, followed by the Student-Newman-Keuls correction. Correlations between protection and immune levels were analyzed using Spearman's rank correlation test. A value of $p < 0.05$ was considered significant.

Results

Immunization protocol

Plasmid DNA and the recombinant vaccinia DIs viruses with the inserted *gag/pol* region of SIVmac239 were constructed as previously described (23). Southern blotting confirmed that all plasmids and viruses had the expected genomic structures, whereas Gag-specific Western blots verified the in vitro expression of SIV Gag protein in rDIsSIV*gag/pol*-infected chick embryo fibroblasts (data not shown). In this study we opted to use the three-injection regimen for DNA immunization. Because we found that both the three- and five-injection DNA immunization strategies resulted in similar levels of T cell immunities (23). A total of 19 cynomolgus macaques were divided into four groups (Fig. 1). Group 1 macaques (prime-boost group of five macaques numbered M1 to M5) received three i.m. injections (2.5 mg) of each type of SIV*gag/pol* DNA at 8-wk intervals, followed by two injections of 10^8 PFU of rDIsSIV*gag/pol*. Group 2 macaques (DNA group of five macaques numbered M6, M7, and M14 through M16) received three i.m. injections of the same dose of each type of SIV*gag/pol* DNA at

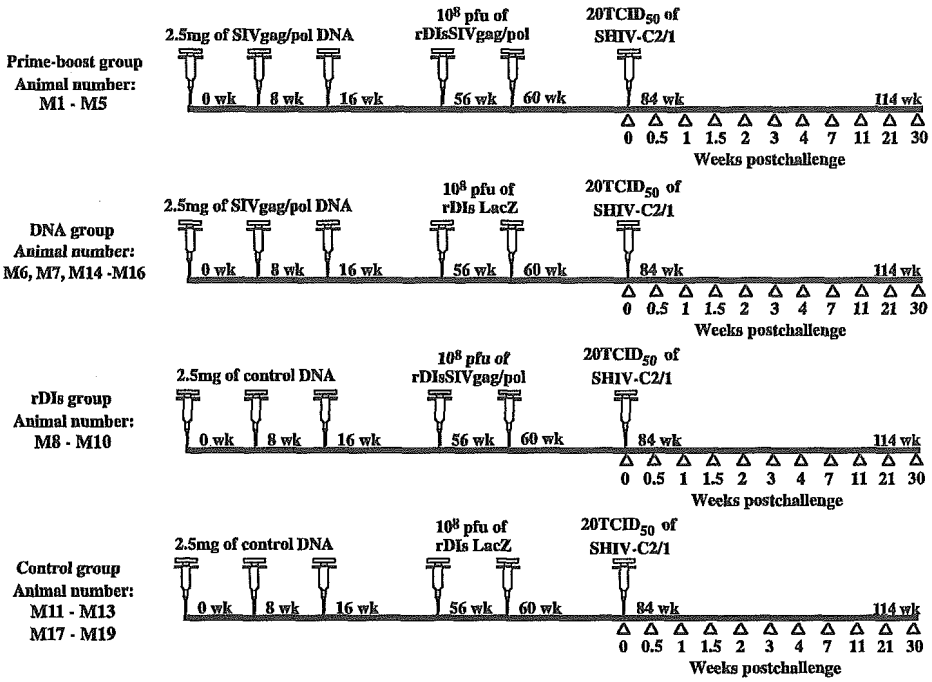

FIGURE 1. Scheme for immunization and viral challenge. Nineteen macaques were divided into four experimental groups and immunized with 2.5 mg of plasmid DNA at weeks 0, 8, and 16, then immunized with 10^8 PFU of rDIs at weeks 56 and 60. Twenty-four weeks after the final immunization, macaques were challenged with 20 $TCID_{50}$ of SHIV.

8-wk intervals, followed by two injections of 10^8 PFU of rDIs-*LacZ*. Group 3 macaques (rDIs group of three macaques numbered M8 through M10) received three i.m. injections of control DNA pcDNA3.1$^-$ at 8-wk intervals, followed by two injections of 10^8 PFU of rDIsSIV*gag/pol*. Group 4 (control group of six macaques numbered M11 through M13 and M17 through M19) received three i.m. injections of control DNA, followed by two injections of 10^8 PFU of rDIsLacZ. Twenty-four weeks after the second booster inoculation, the macaques were i.v. challenged with 20 $TCID_{50}$ of pathogenic SHIV-C2/1, which were obtained by serum passages of SHIV-89.6. The effects of prime-boost vaccination with DNA and vaccinia DIs on protective immune induction were monitored for 30 wk, then animals were autopsied.

Induction of cellular and humoral immune responses specific for SIV Gag

We first analyzed the induction of cellular immunity by detecting the SIV Gag-specific IFN-γ ELISPOT activities of macaque PBMC after the first and third DNA primings and the first boosting of recombinant DIs in each animal (Fig. 2). A regimen of three consecutive immunizations with SIV*gag/pol* DNA induced 3- to 4-fold higher IFN-γ SFC than did a single immunization in the prime-boost and DNA groups ($p < 0.05$; Fig. 2, *A* and *B*). The numbers of IFN-γ-producing SFC increased ~8- to 9-fold after booster immunization with rDIsSIV*gag/pol* in the prime-boost group ($p < 0.01$; Fig. 2*C*). In contrast, no such increase was seen after booster immunization with rDIsLacZ in the DNA group (Fig. 2*C*). Macaques immunized with control DNA followed by rDIs-SIV*gag/pol* (rDIs group) generated higher IFN-γ SFC than the DNA group ($p < 0.01$; Fig. 2, *B* and *C*). At no point in the course of immunization was Gag-specific IFN-γ SFC detected in the control group. Collectively, our findings show that the DNA/rDIs prime-boost immunization efficiently induced immunodeficiency virus-specific ELISPOT activity in macaques.

To substantiate the induction of cellular immunity specific for SIV Gag, intracellular IFN-γ staining was performed using PBMC after the first booster immunization with rDIs (Fig. 3). Of the four groups tested, the prime-boost group showed the highest frequency of IFN-γ-producing $CD4^+$ and $CD8^+$ T cells. The frequencies of Gag-specific IFN-γ-producing $CD8^+$ and $CD4^+$ T cell responses to Gag peptides in the prime-boost group ranged from 0.51 to 1.22% with an average of 0.82%, and from 0.37 to 0.63% with an average of 0.46%, respectively. The expression of IFN-γ-producing $CD8^+$ and $CD4^+$ T cells immunized with either SIV*gag/pol* DNA (average of $CD8^+$ T cells, 0.095%; average of $CD4^+$ T cells, 0.015%) or rDIsSIV*gag/pol* (average of $CD8^+$ T cells, 0.27%; average of $CD4^+$ T cells, 0.05%) was apparently weak (Fig. 3). Therefore, as observed for the induction of the SIV Gag-specific ELISPOT activities, the prime-boost group proved to be the most efficient of the four animal groups tested at inducing Ag-specific intracellular IFN-γ cytokine staining.

To test for the induction of humoral immunity, we assessed the SIV Gag-specific IgG titers in the animals of each group (Fig. 4). Despite the elevation of Ab titers after the first immunization with SIV*gag/pol* DNA, no enhanced responses were observed after two serial immunizations with the DNA (Fig. 4*A*). However, although the titers did not exceed 2000, enhanced Ab responses were observed after booster immunization with rDIsSIV*gag/pol*. In summary, these results show that the prime-boost vaccine with DNA/rDIs predominantly elicits SIV Gag-specific cellular immune responses in immunized animals.

Enhancement of SIV-specific T cell and humoral immune responses after viral challenge

Twenty-four weeks after the second immunization with rDIs, macaques were challenged with highly pathogenic SHIV. As shown in Fig. 5*A*, Gag-specific IFN-γ SFC levels decreased on the day of challenge in all vaccinated groups, but the increase observed in the numbers of the SFC after SHIV challenge varied among the groups. The most pronounced increase was seen in the prime-boost group, with the average number of Gag-specific IFN-γ-producing cells increasing from 288/million PBMC on the day of challenge to 1124 ($p < 0.01$) 3 days after challenge. The DNA group increased from an average of 104 to 282 ($p < 0.01$), and the rDIs group from 114 to 347 ($p < 0.05$). No significant increases were noted in the control group.

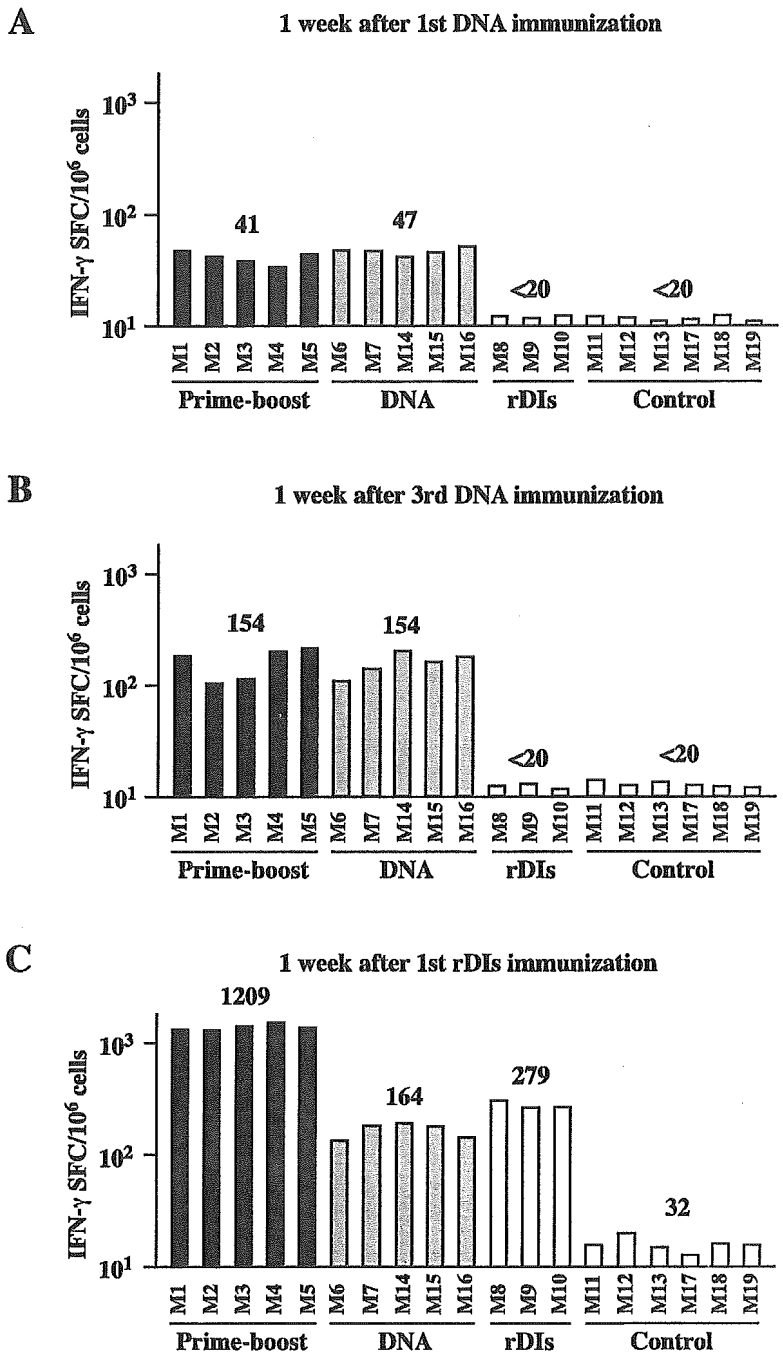

FIGURE 2. Frequency of SIV Gag-specific IFN-γ-producing cells in immunized macaques. Values are provided at 1 wk after the first DNA immunization (*A*), 1 wk after the third DNA immunization (*B*), and 1 wk after rDIs immunization (*C*). The numbers above the data bars represent the geometric means of the SFC levels in each group. Experimental groups and animal numbers are indicated at the bottom of the graph.

Intracellular IFN-γ staining of $CD8^+$ and $CD4^+$ T cells was also performed to assess any enhancement in immunodeficiency virus-specific immune responses (Fig. 5*B*). On the day of challenge, populations of Gag-specific IFN-γ-producing $CD8^+$ T cells in the prime-boost group averaged 0.32%, and populations of $CD4^+$ T cells averaged 0.11%. Three days after viral challenge, the average for Ag-specific IFN-γ-producing $CD8^+$ T cells rose to 0.61%, and that for $CD4^+$ T cells to 0.38%. Gag-specific IFN-γ-producing $CD8^+$ T cells averaged 0.18% for the DNA group and 0.25% for the rDIs group on the day of challenge, with those averages rising to 0.28 and 0.39%, respectively, by 3 days after challenge. Furthermore, the averages for Gag-specific $CD4^+$ T cells in the DNA and rDIs groups rose from 0.08 and 0.10 to 0.14 and 0.23%, respectively. The number of Ag-specific IFN-γ-producing $CD8^+$ and $CD4^+$ T cells in the control group was not affected by viral challenge. Thus, compared with the other three groups of animals, the prime-boost group showed the most significant enhancement of Ag-specific cellular immune responses after viral challenge, suggesting that Gag-specific memory T cell responses may be efficiently generated in animals by immunization with the prime-boost vaccine regimen.

To test the kinetics of humoral immune responses after SHIV challenge, we measured serum IgG titers to SIV Gag and SHIV 89.6P Env in all animals of each group (Fig. 4, *A* and *B*). The SIV Gag-specific IgG titers in all vaccinated animals were rapidly elevated and reached peak levels within 4 wk after challenge (Fig. 4*A*). The peak IgG titers in the prime-boost, DNA, and rDIs groups averaged 14,520 ± 2,508, 5,240 ± 1,099, and 8,400 ± 1,114,

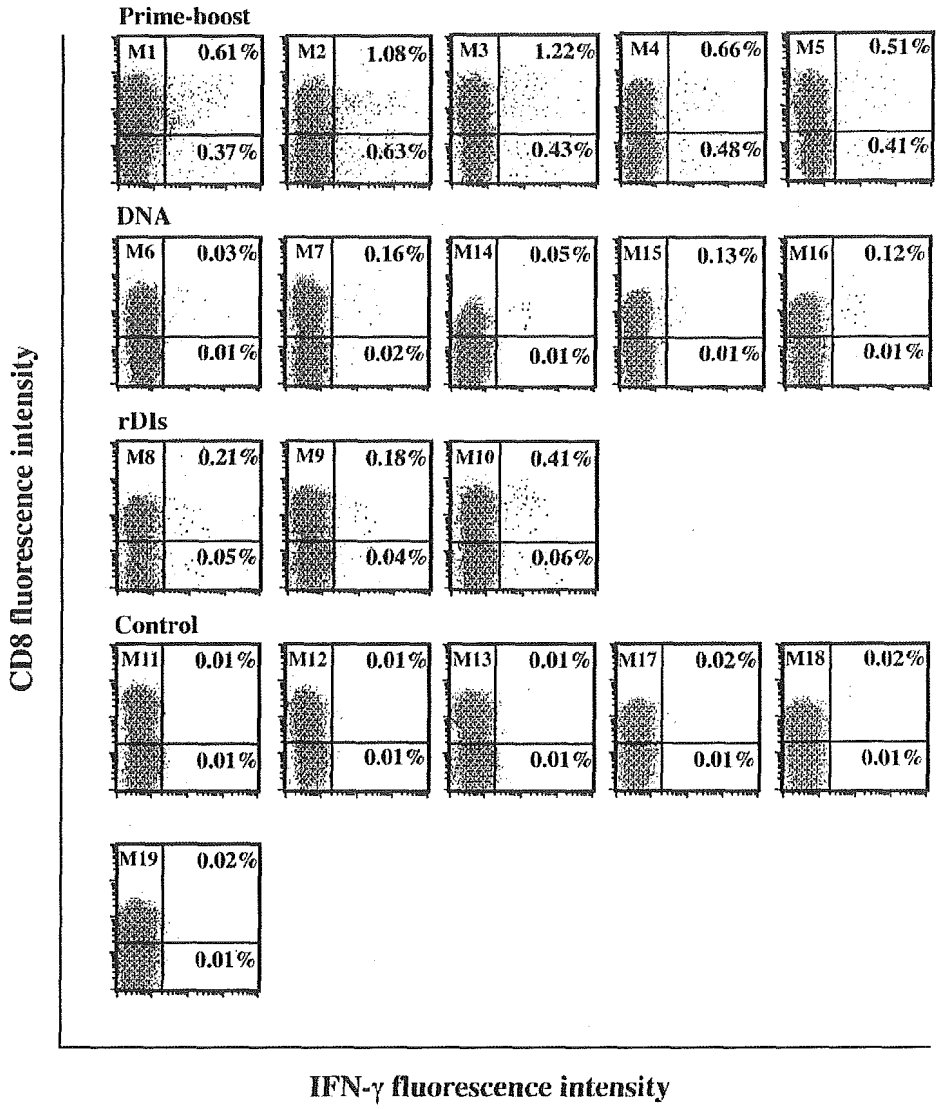

FIGURE 3. Flow cytometric analysis of SIV Gag-specific IFN-γ-producing $CD8^+$ T cells. One week after rDIs boost immunization, freshly isolated PBMC were stimulated with 0.2 μM pooled SIV Gag peptides and stained for anti-CD3, -CD8, and -IFN-γ. Twenty thousand lymphocyte-gated events were acquired. Upper and lower quadrants represent the frequencies of $CD8^+$ IFN-γ^+ and $CD4^+$ IFN-γ^+ T cells, respectively. Numbers indicate the percentage of cells in each quadrant.

respectively, with the increase in the prime-boost group reaching statistical significance ($p < 0.01$), compared with that in the DNA and rDIs groups. The Env-specific IgG appeared by 4 wk after challenge and reached peak levels between 7 and 11 wk. The peak IgG titers in the prime-boost, DNA, and rDIs groups averaged 5,200 ± 1,839, 3,180 ± 701, and 4,533 ± 833, respectively. Both the SIV Gag- and Env-specific IgG titers in the three vaccinated groups maintained high levels and persisted throughout the challenge period. In contrast, no IgG response to Gag and Env was detected in the control group. High titers of Env-specific IgG, but only very low levels of neutralization Ab responses to SHIV-C2/1, were induced in the DNA- and rDI-vaccinated groups (Fig. 4*C*). In contrast, the prime-boost macaques, especially M1, had high levels of neutralization Ab responses (viral neutralization >70%). Thus, these results show that the prime-boost vaccine with DNA/rDIs predominantly elicits SIV Gag-specific humoral responses in immunized animals and generates SHIV Env-specific binding and neutralization Abs after challenge with SHIV.

Macaques of the prime-boost group control plasma viral load and block $CD4^+$-T cell depletion

As noted above, the five macaques in the prime-boost group developed Ag-specific positive immunity after viral challenge. In these macaques, plasma viral loads were most attenuated and $CD4^+$ T cell counts best maintained in peripheral blood (Fig. 6). Peak viral loads occurred 2 wk after challenge in each group. The geometric means of the viral RNA copies were 1.1×10^7 copies in the prime-boost group, 4.7×10^7 copies in the DNA group, 4.1×10^7 copies in the rDIs group, and 4.5×10^7 copies in the control group (Fig. 6*A*). The difference observed in geometric mean peak viremia for the prime-boost and rDIs groups was significant ($p < 0.05$). Levels of peak viremia in the rDIs and control groups did not significantly differ. The peak viral loads in each had decreased by 7 wk after challenge, and the geometric means of the viral RNA copies from 7 to 30 wk were 8.1×10^3 copies (ranging from 7.1×10^3 to 9.4×10^3 copies) in the prime-boost group, 1.1×10^6 copies (ranging from 2.5×10^5 to 6.6×10^6 copies) in the DNA group, 7×10^4 copies (ranging from 5.3×10^4 to 1.1×10^5 copies) in the rDIs group, and 6.8×10^6 copies (ranging from 2.0×10^6 to 5.2×10^7 copies) in the control group (Fig. 6*A*). From 7 to 30 wk, the differences in the geometric means of the viral RNA copies between prime-boost and DNA groups ($p < 0.01$), prime-boost and rDIs groups ($p < 0.01$), and DNA and rDIs groups ($p < 0.01$) vs DNA and control groups ($p < 0.05$) were significant.

Two weeks after challenge, both DNA and control groups showed a serious depletion of $CD4^+$ T cells (to <50 cells) and a corresponding increase in viral RNA. In contrast, the prime-boost

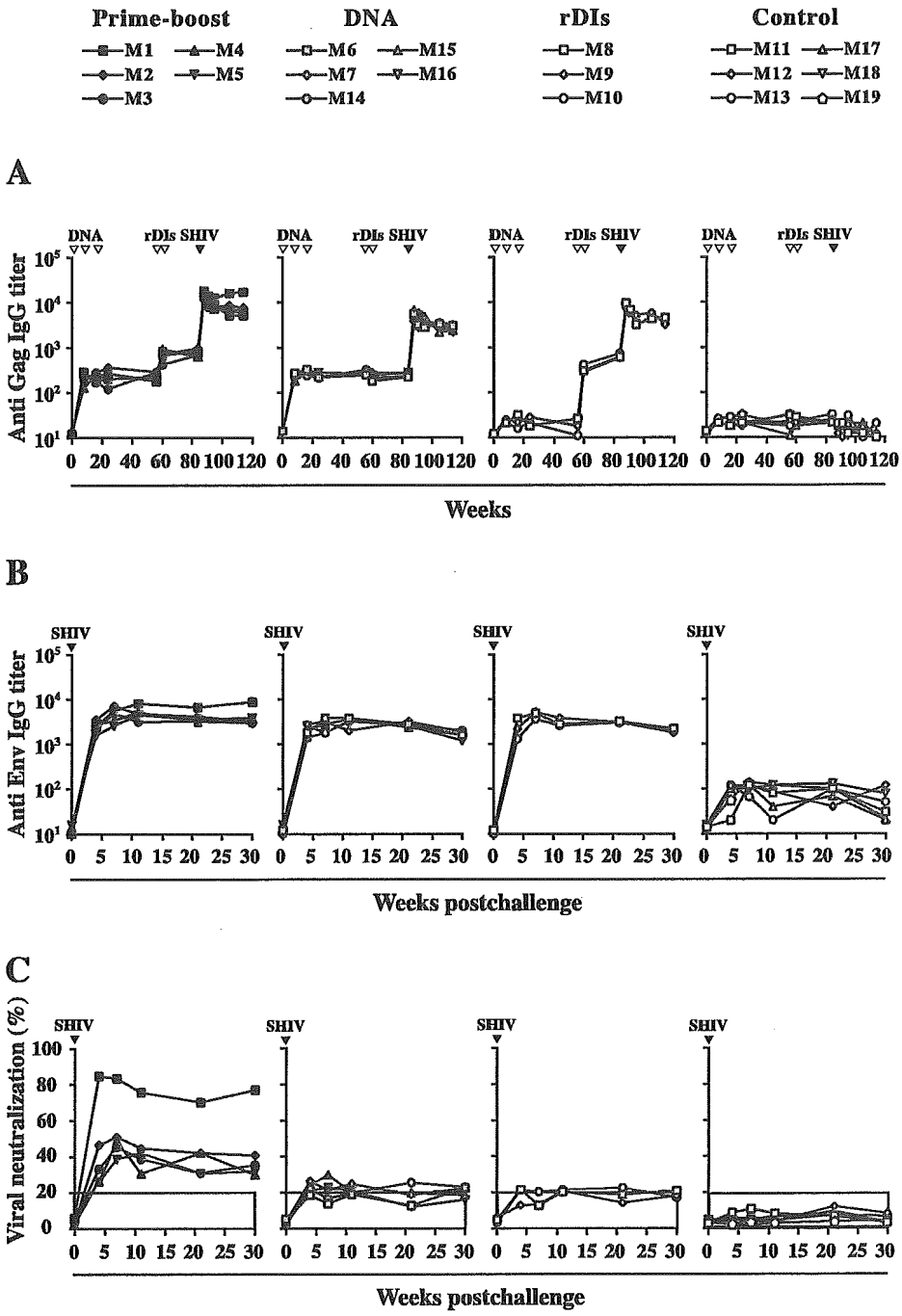

FIGURE 4. Kinetics of serum IgG titers specific to SIV Gag and SHIV 89.6P Env. *A*, SIV p27 Gag- and Env-specific IgG titers after immunization and after challenge. *B*, SHIV 89.6P Env-specific IgG titers. *C*, SHIV-specific neutralization responses. End-point titers of Gag- and Env-specific serum IgG and the percentage of SHIV-specific neutralization responses were measured at each time point. Results represent the average titer and percentage of the average viral neutralization value.

group maintained its $CD4^+$ T cell counts up to 30 wk after challenge (Fig. 6*B*). Four of the five macaques (M2–5) in the prime-boost group exhibited a gradual decrease in $CD4^+$ T cell counts; however, the macaques maintained an average of 254–303 cells from 2 to 30 wk after challenge. The one remaining macaque in the group (M1) maintained an average of 833 $CD4^+$ T cells (ranging from 630 to 1230 cells) and exhibited levels of viral RNA (<500 copies) that were undetectable except when peak viremia was reached at 2 wk (5.7×10^7 copies) and transient viral replication occurred at 7 wk (1.5×10^4 copies; Fig. 6, *A* and *B*).

To characterize the changes in the $CD4^+$ T cell subset in peripheral blood of each group after SHIV challenge, we used flow cytometric analysis to obtain an absolute count and to distinguish among the $CD29^+$, $CD45^+$, and $CD28^+$ cell subpopulations (Fig. 6, *C–E*). By 2 wk after challenge, a sharp decrease in the $CD29^+$ subset of $CD4^+$ T cells was seen in the DNA, rDIs and control groups (Fig. 6*C*). From 2 to 30 wk after challenge, the average number of this subset of cells in the DNA, rDIs, and control groups was 1.21% (ranging from 0.79 to 2.01%), 2.14% (ranging from 1.80 to 3.59%), and 1.03% (ranging from 0.55 to 1.89%), respectively. Similarly, the $CD45RA^+$ subset of $CD4^+$ T cells in the three groups rapidly declined by 2 wk after challenge, with the average of naive cells from 2 to 30 wk being 1.04% (ranging from 0.72 to 1.32%) in the DNA group, 2.83% (ranging from 1.04 to 4.78%) in the rDIs group, and 0.88% (ranging from 0.34 to 1.34%) in the control group (Fig. 6*D*). In contrast, the prime-boost group maintained the highest frequencies of both the $CD29^+$ subset, ranging from 8.0 to 9.63% with an average of 8.82% (Fig. 6*C*), and

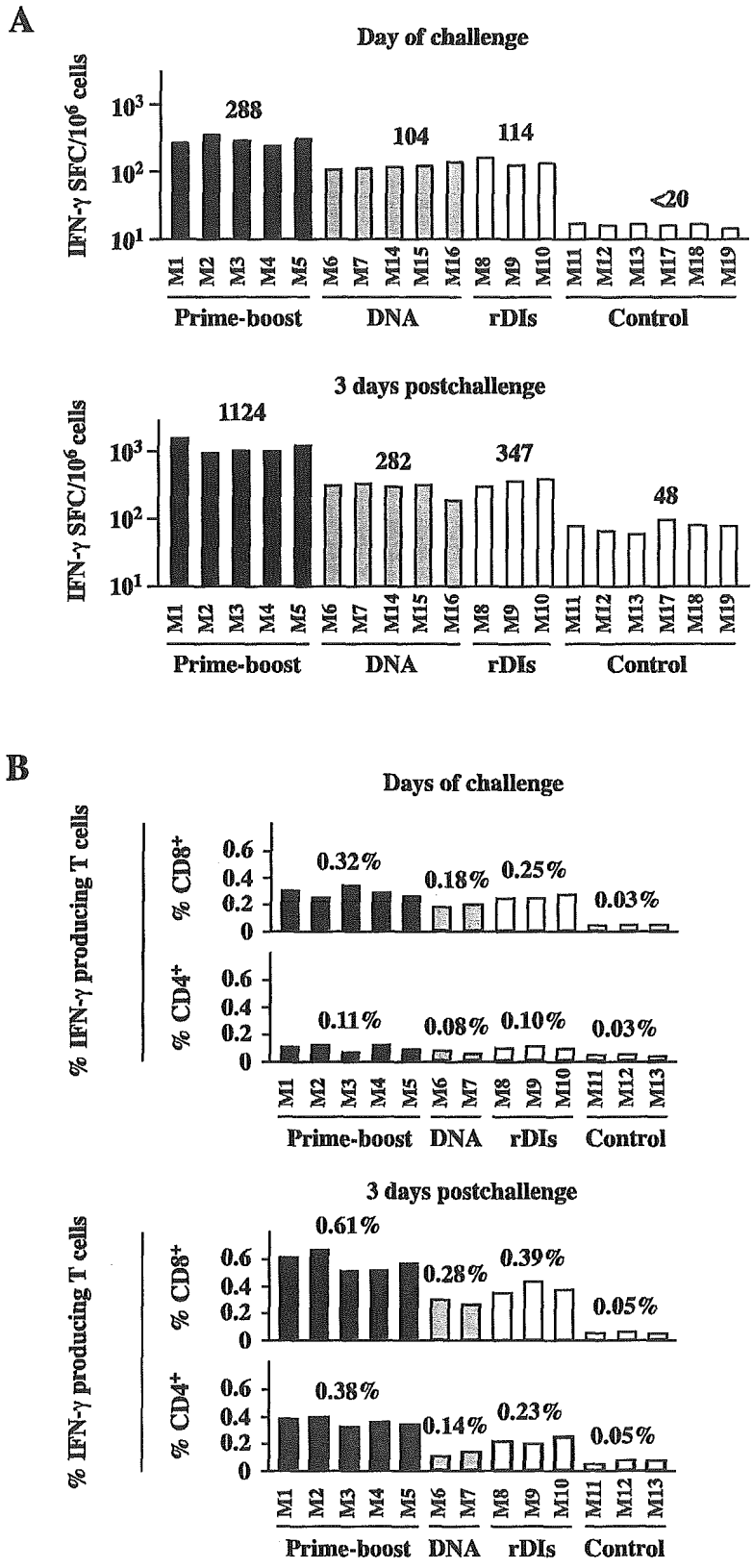

FIGURE 5. Comparison of IFN-γ ELISPOT activity and intracellular IFN-γ-producing T cells specific for SIV Gag in PBMC before and after viral challenge. *A*, ELISPOT activity. The numbers above the data bars represent the geometric means of SFC levels in each group. *B*, Intracellular IFN-γ-producing T cells. On the day of SHIV challenge and 3 days after SHIV challenge, freshly isolated cells were stimulated with SIV Gag peptides and stained for CD3, CD8, and IFN-γ. Numbers represent the percent average of the $CD4^+$ and $CD8^+$ T cell frequencies.

the $CD45^+$ subset, ranging from 6.29 to 9.16% with an average of 7.59% (Fig. 6, *C* and *D*). Flow cytometric analyses also revealed that the number of $CD4^+$ T cells expressing the costimulatory molecule CD28 rapidly dropped in the DNA, rDIs, and control groups by 2 wk after challenge (Fig. 6*E*). The average of $CD4^+CD28^+$ T cells from 2 to 30 wk after challenge in the DNA, rDIs, and control groups was 0.74% (ranging from 0.23 to 1.12%), 1.66% (ranging from 1.01 to 2.6%), and 0.91% (ranging from 0.61 to 1.13%), respectively. In contrast, $CD28^+CD4^+$ T cells in the prime-boost group ranged from 5.27 to 7.26%, with an average of

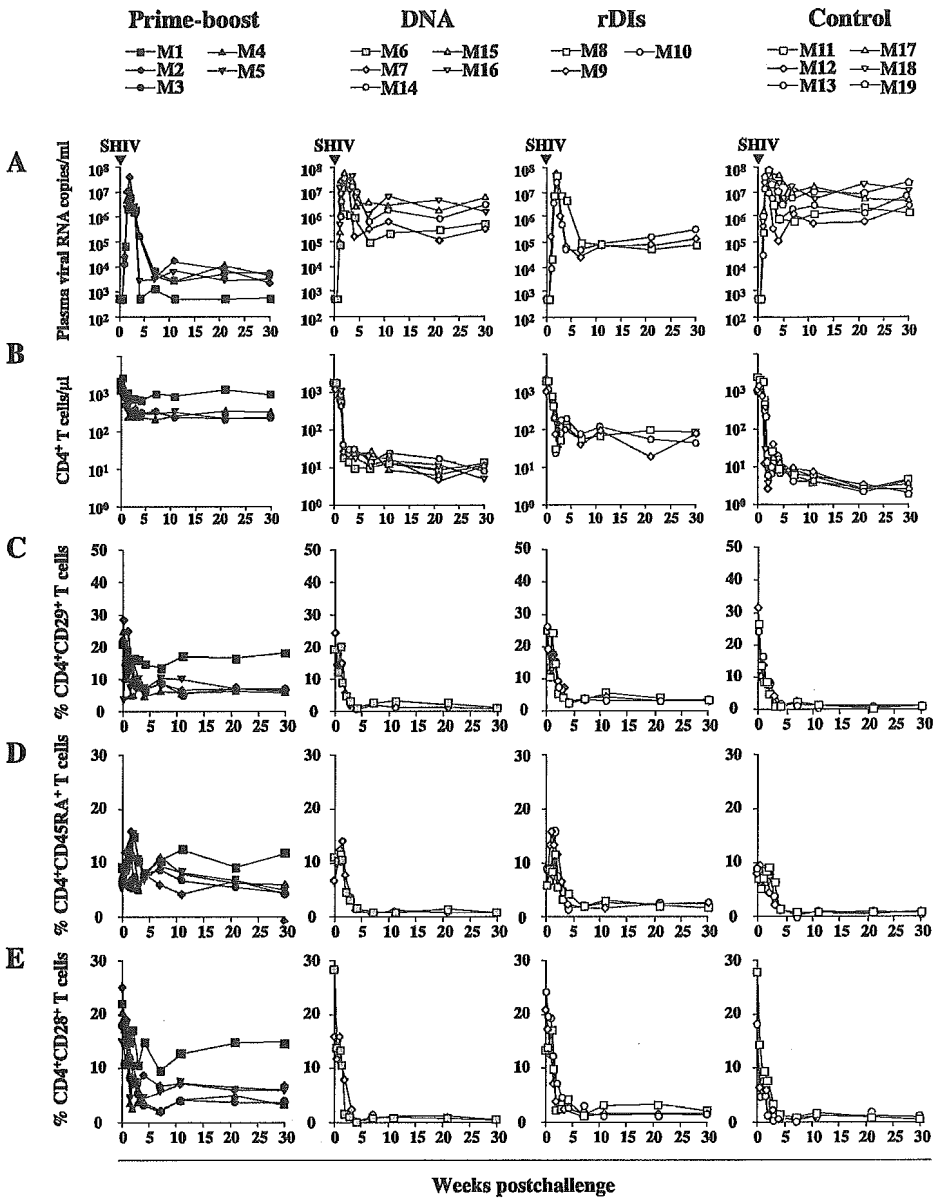

FIGURE 6. Kinetics of viral loads, $CD4^+$ T cell counts, and subpopulations of $CD4^+$ T cells in experimental groups after SHIV challenge. *A*, Plasma viral loads. Plasma viral loads were measured using the real-time PCR system. Levels <500 copies/ml were considered undetectable in this system. *B*, $CD4^+$ T cell counts. Whole blood was stained for CD3, CD4, and CD8 Abs, and $CD4^+$ T cell counts were determined using flow cytometry. *C*, $CD4^+CD29^+$ T cells. *D*, $CD4^+CD45RA^+$ T cells. *E*, $CD4^+CD28^+$ T cells. $CD4^+$ T cell subpopulations were not reduced in the prime-boost animal group.

6.75%. Thus, the prime-boost group maintained $CD29^+$, $CD45RA^+$, and $CD28^+$ cell subpopulations in $CD4^+$ T cells after viral challenge.

Controls of viremia and stability of $CD4^+$ blood lymphocytes correlate with Gag-specific IFN-γ SFC and neutralization Ab responses

Because positive immune responses were detected in the animals immunized with the prime-boost vaccine of DNA/vaccinia DIs, we examined whether any immune responses correlated with the positive immunities using Spearman's rank correlation test (Fig. 7). The set-point levels of plasma viral RNA and $CD4^+$ T cell counts 7 wk after challenge significantly correlated with the Gag-specific IFN-γ SFC levels 3 days after challenge (plasma viral RNA levels vs Gag-specific IFN-γ SFC levels: Rs = 0.850, $p = 4.07 \times 10^{-6}$; $CD4^+$ T cell counts vs Gag-specific IFN-γ SFC levels: Rs = 0.968, $p = 1.10 \times 10^{-11}$; Fig. 7*A*). Interestingly, there was less correlation between the same set-point plasma viral RNA levels and $CD4^+$ T cell counts and the neutralization Ab responses 7 wk after challenge (plasma viral RNA levels vs percent viral neutralization: Rs = 0.796, $p = 4.53 \times 10^{-5}$; $CD4^+$ T cell counts vs percent viral neutralization: Rs = 0.851, $p = 3.93 \times 10^{-6}$). No correlation at all was observed between positive immune responses and anti-Gag and anti-Env Ab titers (data not shown).

Discussion

It is believed likely that HIV-specific immune responses are associated with a decline in viral load and $CD4^+$ T cell maintenance. Our current study using the macaque model suggests that the prime-boost regimen, that is, priming with SIV*gag/pol* DNA followed by boosting with rDIsSIV*gag/pol*, modifies pathogenic SHIV infection. Furthermore, when the relationship between protection and the levels of immune responses was analyzed, we found that Gag-specific IFN-γ T cells showed a strong correlation and neutralization responses a weaker correlation with the suppression of plasma viral RNA levels and maintenance of $CD4^+$ T cell counts. These results accord with previous reports associating

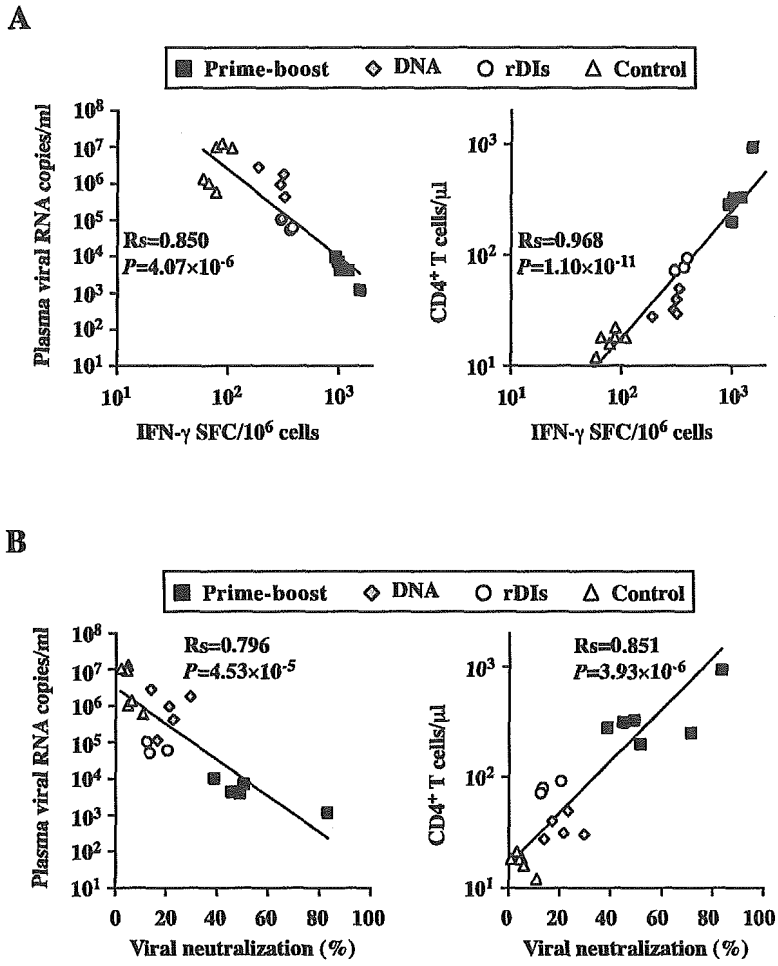

FIGURE 7. Correlations between protection and immune responses. *A*, The correlations between the decline in plasma viral RNA and the increased number of Gag-specific IFN-γ SFC, and between $CD4^+$ T cell counts and Gag-specific IFN-γ SFC. *B*, Correlations between the decline in plasma viral RNA and increased neutralization Ab responses, and between $CD4^+$ T cell counts and neutralization Ab responses. Correlations are calculated using Spearman's rank correlation test.

viral control with cellular immune responses in animals immunized with a prime-boost vaccination of either DNA/MVA (11) or cytokine-augmented DNA (36) encoding *gag* and *env* genes, followed by SHIV challenge. Neutralization Ab production was also detected in the animals (11, 36). Our new observations in vaccine research include the following: 1) Because positive immune responses better correlated with T cell than neutralization responses, it is probable that control of the plasma viral load and $CD4^+$ cell counts was achieved by virus-specific cellular immune responses. 2) Although our vaccine target was only Gag in this strategy, neutralization titers were detected in the prime-boost group that were higher than those induced in animals immunized with DNA, rDIs, or vector controls alone. These higher titers of the neutralization Ab responses against challenge virus might account for the presence of a high number of $CD4^+$ T cells in prime-boost animals (Fig. 6*B*) and might be associated with the production of neutralization Ab. It may, therefore, be reasonable to conclude that anti-Env neutralization Abs were effectively induced in the animals after SHIV challenge. Thus, we suggest that not only cellular responses, but also neutralizing Ab responses, elicited by the challenge virus may play a role in the pathogenesis of HIV/AIDS in the macaque model. 3) This vaccination regimen consisted of DNA and a nonreplicating vaccinia virus DIs, which is very safe even in immunodeficient states. Although other highly attenuated vaccinia strains replicate under synchronized viral infections to mammalian cells (37, 38), the DIs does not replicate in any mammalian cells tested because of natural big deletion of the genome (22, 23, 39). Thus, DIs vaccination eliminates the risk of a disseminated or progressive vaccinia viral infection in the immunocompromised, HIV-infected individual. Therefore, the DNA/DIs vaccine will be most safe in mammalians and may be suitable for therapeutic vaccine.

Recently, we demonstrated that priming with SIV*gag/pol* DNA, followed by boosting with rDIsSIV*gag/pol* generated both Th1-type $CD8^+$ and $CD4^+$ T cell responses specific for SIV Gag, resulting in the protection of immunized mice from a wild-type vaccinia virus recombinant expressing SIV Gag and Pol (23). Our previous mouse and macaque results (23, 40) (Fig. 6) showed that DNA alone was not as effective at inducing positive immunity in the macaque AIDS model as had been reported by others (11, 36). This discrepancy may depend on differences in DNA preparation, for example, whether the target HIV DNA was optimized to the human codon.

Although the exact immune mechanism responsible for protection from viral infection is not yet fully understood, both Ag-specific $CD4^+$ and $CD8^+$ T cell responses were clearly enhanced by viral infection in the prime-boost-immunized animals that exhibited a pronounced attenuation of plasma viral load. Our finding that challenge with the highly pathogenic SHIV virus enhances cellular immunity confirms the results of a recent study (41). It has been demonstrated that HIV-specific $CD8^+$ T cell responses play an important role in controlling viral replication by cytolysis and cytokine and/or anti-virus factor production (1, 2, 3, 42, 43). Others have also documented that HIV-specific $CD4^+$ T cell responses contribute to virus control or the slowing of disease progression (44–46). The critical role played by $CD4^+$ T cell responses against viral infections was also reported in studies of murine

lymphatic choriomeningitis viral infection (47) and CMV immunity in bone marrow transplant recipients (48). DNA/poxvirus prime-boost vaccination induced a high frequency and a high avidity of $CD8^+$ cytotoxic T lymphocyte populations (49), with the magnitude of HIV/SIV-specific $CD4^+$ and/or $CD8^+$ T lymphocyte responses in the course of infection inversely correlating with the viral load (50, 51). In addition, MHC class I molecules loading CTL epitopes may help control viral replication (52–56). The exact mechanisms underlying protective immune responses against HIV-1 remain a subject of debate; however, the above studies suggest that the simultaneous induction after vaccination of both Ag-specific $CD8^+$ and $CD4^+$ T cell responses may make it possible to attenuate immunodeficient viral infection. In this study we showed the efficacy of the prime-boost vaccination by monitoring IFN-γ ELISPOT, intracellular IFN-γ, and Ab responses. In the prime-boost group, boosting with rDIsSIV*gag/pol* induced ELISPOT responses (average of 1209 SFC) almost 10-fold higher than those induced by SIV*gag/pol* DNA (average of 154 SFC). In addition, intracellular IFN-γ staining revealed that the prime-boost vaccination generated high levels of Gag-specific intracellular IFN-γ-producing $CD8^+$ T cells (average, 0.82%; range, 0.51–1.22%) as well. However, lower Gag-specific T cell responses were observed in macaques vaccinated with either SIV*gag/pol* DNA or rDIsSIV*gag/pol* alone than with the prime-boost regimen. In contrast to the strong Gag-specific T cell responses generated by the prime-boost vaccination, humoral responses specific for the same Ag were apparently low throughout the course of immunization. Although the peak IgG titers in the prime-boost group were observed after the first or second boosting with rDIsSIV*gag/pol*, Ab titers remained low. These results are in line with our previous study using the mouse model (23), suggesting that our prime-boost vaccine immunodominantly generates SIV Gag-specific cellular responses in macaques.

Monitoring ELISPOT and intracellular IFN-γ T cell responses specific for Gag revealed that responses decreased at the time of challenge with pathogenic SHIV, but then rapidly recovered. Gag-specific IFN-γ ELISPOT responses in the prime-boost group averaged 288 SFC on the day of challenge and increased to 1124 SFC on day 3 after challenge. The population of intracellular IFN-γ-producing $CD8^+$ and $CD4^+$ T cells specific for Gag also increased from an average of 0.32 to 0.61% and from an average of 0.11 to 0.38%, respectively, suggesting that our prime-boost vaccine generated a high frequency of very responsive $CD4^+$ and $CD8^+$ memory T cells that immediately reactivated sufficient levels of the Ag-specific immune responses against the SHIV Ag. Furthermore, a kinetic study of plasma viral loads and counts of $CD4^+$ T cells after challenge with SHIV revealed different patterns for each group. Although peak plasma viral loads were observed 2 wk after challenge in all groups, the number of plasma RNA copies peaking at that time in the prime-boost group were ~5-fold lower than in other groups, with numbers remaining depressed during the period extending from 7 to 30 wk after infection. However, high $CD4^+$ T cell counts were maintained in the prime-boost group. These results suggest a correlation between both plasma viral loads and the maintenance of high $CD4^+$ T cell counts and T cell response levels.

With regard to safety of vaccinia DIs as a vaccine vector, its viral replication occurs only in chick embryo fibroblasts, not in any mammalian cell lines tested (22, 24–26, 57). Because a vaccine regimen combining DNA and a defective DIs vector would not run the risk that the virus used as vector might replicate and disseminate, it would pose less of a risk to a severely immunocompromised host. Furthermore, in this study using the macaque model, we demonstrated that the cellular immune responses generated by the prime-boost vaccination were higher than those induced by vaccination with either DNA or rDIs alone and that response levels correlated to plasma viral loads and $CD4^+$ T cell counts after challenge with pathogenic SHIV. In summary, these results demonstrate that the new prime-boost regimen safely and effectively elicits anti-immunodeficiency viral immunity, suggesting its promise as a potential vaccine against HIV-1 infection as well as against HIV-induced disease progression.

Current macaque models of HIV, SIV, and SHIV may fall short of precisely mirroring human HIV infection. In some macaque HIV/AIDS models, SIVmac239 has been targeted as a desirable challenge virus, because it is a typical CCR5-tropic SIVmac and can cause both chronic and progressive disease in macaques (41, 58, 59). However, the virus is very difficult to neutralize and also very difficult to clear even from animals that have been previously immunized with homologous recombinant vector-based vaccines (41, 58, 59). Only live attenuated SIV has been reported to control SIVmac239 (T. Allen, Global HIV Vaccine Enterprise Meeting, Washington, October 21, 2004). Although there may be no macaque model suitable for evaluating the efficacy of an SIV or HIV experimental immunogen, in this study we clearly showed that vaccination with an SIV experimental immunogen consisting of SIV*gag/pol* DNA and replication-defective rDIsSIV*gag/pol* caused a pronounced attenuation of the infection caused by a highly pathogenic variant of SHIV-C2/1 in all five macaques tested. SHIV-C2/1, used as challenge virus, is a variant of SHIV 89.6. Because SHIV89.6 does not induce both a marked decline in $CD4^+$ cells and a high level of plasma viral load in cynomolgus macaques, we passaged serum from virus-infected cynomolgus macaques. The variant was obtained by the serum passages using cynomolgus macaques inoculated with SHIV89.6, and it induced high levels of viremia ($1–10 \times 10^7$ viral RNA copies/ml) and marked $CD4^+$ T cell depletion (<10 cells/μl) within 2 and 3 wk after viral inoculation (30, 31, 39). Furthermore, genomic study revealed 16 mutations of genomic DNA and 15 amino acid mutations in the Env region of parental virus. Thus, the cynomolgus AIDS model challenged with SHIV-C2/1 may represent primary HIV-1 infection in humans. These results should prove useful in determining how potent the new prime-boost vaccine regimen might be at eliciting anti-immunodeficiency virus immunity.

HIV-1 has been reported to preferentially infect $CD45RO^+CD4^+$ T cells in the early stages of infection, with the number of $CD45RA^+CD4^+$ T cells declining in later stages (60–62). Furthermore, the loss of this subpopulation of $CD4^+$ T cells during the early phase of immunodeficiency virus infection correlates to disease progression (63, 64), whereas the low $CD45RA^+CD4^+$ T cell levels in the late stages of infection correlate with an increased risk of death (65–67). The levels of $CD4^+$ T cells expressing the $CD28^+$ molecule have also been demonstrated to correlate with disease progression (68, 69). To confirm the effect of prime-boost immunity after SHIV challenge, we analyzed the kinetics of $CD4^+$ T cells expressing $CD29^+$, $CD45RA^+$, and $CD28^+$ molecules. We observed that the prime-boost group maintained the subpopulations of $CD4^+$ T cells throughout the course of infection, with an average of 8.82% $CD29^+$ cells, 7.59% $CD45\ RA^+$ cells, and 6.75% $CD28^+$ cells. In contrast, $CD4^+$ T cell populations in the other DNA and rDIs groups were reduced to <3%. These results suggest that immunization with the new prime-boost regimen induces protective immunity while maintaining the levels of the various $CD4^+$ T cell subpopulations.

In summary, our study has shown that the vaccine strategy that primes with DNA and then boosts with the replication-defective

vaccinia virus DIs generates both $CD4^+$ and $CD8^+$ T cell responses specific for SIV Gag, resulting in protection of the immunized macaques from pathogenic SHIV. However, it remains to be elucidated whether the *gag/pol*-encoding vaccine may elicit a protective effect against various viral challenges, such as CCR5-tropic viruses and other primary viruses. Nonetheless, this new regimen's twin merits of safety and efficacy position it as a promising vaccine candidate against HIV-1 infection as well as against HIV-induced disease progression.

Acknowledgments

We thank Dr. Naoto Yoshino (Iwate Medical University, Iwate, Japan) for technical support and advice.

Disclosures

The authors have no financial conflict of interest.

References

1. Koup, R. A., J. T. Safrit, Y. Cao, C. A. Andrews, G. McLeod, W. Borkowsky, C. Farthing, and D. D. Ho. 1994. Temporal association of cellular immune responses with the initial control of viremia in primary human immunodeficiency virus type 1 syndrome. *J. Virol.* 68: 4650–4655.
2. Ogg, G. S., X. Jin, S. Bonhoeffer, P. R. Dunbar, M. A. Nowak, S. Morand, J. P. Segal, Y. Cao, S. L. Rowland-Jones, V. Cerundolo, et al. 1998. Quantitation of HIV-1 specific cytotoxic T lymphocytes and plasma load of viral RNA. *Science* 297: 2103–2106.
3. Ogg, G. S., S. Kostense, M. R. Klein, S. Jurriaans, D. Hamann, A. J. McMichael, and F. Miedema. 1999. Longitudinal phenotypic analysis of human immunodeficiency virus type 1-specific cytotoxic T lymphocytes: correlation with disease progression. *J. Virol.* 73: 9153–9160.
4. Wagner, R., B. Leschonsky, E. Harrer, C. Paulus, C. Weber, B. D. Walker, S. Buchbinder, H. Wolf, J. R. Kalden, and T. Harrer. 1999. Molecular and functional analysis of a CTL epitope in HIV-1 p24 recognized from a long-term nonprogressor: constraints on immune escape associated with targeting a sequence essential for viral replication. *J. Immunol.* 162: 3727–3734.
5. Jin, X., D. E. Bauer, S. E. Tuttleton, S. Lewin, A. Gettie, J. Blanchard, G. E. Irwin, J. T. Safrit, J. Mittler, L. Weinberger, et al. 1999. Dramatic rise in plasma viremia after $CD8^+$ T cell depletion in simian immunodeficiency virus infected macaques. *J. Exp. Med.* 189: 991–998.
6. Betts, M. R., J. Krowka, C. Santamaria, K. Balsamo, K. Gao, G. Mulundu, C. Luo, N. N'Gandu, H. Sheppard, B. H. Hahn, et al. 1997. Cross-clade human immunodeficiency virus (HIV)-specific cytotoxic T-lymphocytes responses in HIV-infected Zambians. *J. Virol.* 71: 8908–8911.
7. Durali, D., J. Morvan, F. Letourneur, D. Schmitt, N. Guegan, M. Dalod, S. Saragosti, D. Sicard, J. P. Levy, and E. Gomard. 1998. Cross-reactions between the cytotoxic T-lymphocytes responses of human immunodeficiency virus-infected African and European patients. *J. Virol.* 72: 3547–3553.
8. McAdam, S., P. Kaleebu, P. Krause, P. Goulder, N. French, B. Collin, T. Blanchard, J. Whitworth, A. McMichael, and F. Gotch. 1998. Cross-clade recognition of p55 by cytotoxic T lymphocytes in HIV-1 infection. *AIDS* 12: 571–579.
9. Kent, S. J., A. Zhao, S. J. Best, J. D. Chandler, D. B. Boyle, and I. A. Rhamsaw. 1998. Enhanced T-cell immunogenicity and protective efficacy of human immunodeficiency virus type 1 vaccine regimen consisting of consecutive priming with DNA and boosting with recombinant fowlpox virus. *J. Virol.* 72: 10180–10188.
10. Robinson, H. L., D. C. Monteriori, R. P. Johnson, K. H. Hanson. M. L. Kalish, J. D. Lifson, T. H. Rizvi, S. Lu, S. L. Hu, G. P. Mazzara, et al. 1999. Neutralizing antibody-independent containment of immunodeficiency virus challenge by DNA priming and recombinant poxvirus booster immunizations. *Nat. Med.* 5: 526–534.
11. Amara, R. R., F. Villinger, J. D. Altman, S. L. Lydy, S. P. O'Neil, S. I. Staprans, D. C. Montefiori, Y. Xu, J. G. Herndon, L. S. Wyatt, et al. 2001. Control of a mucosal challenge and prevention of AIDS by a multiprotein DNA/MVA vaccine. *Science* 296: 69–74.
12. Amara, R. R., F. Villinger, S. I. Staprans, J. D. Altman, D. C. Montefiori, N. L. Kozyr, Y. Xu, L. S. Wyatt, P. L. Earl, J. G. Herndon, et al. 2002. Different patterns of immune responses but similar control of a simian-human immunodeficiency virus 89.6P mucosal challenge by modified vaccinia virus Ankara (MVA) and DNA/MVA vaccines. *J. Virol.* 76: 7625–7631.
13. Tang, Y., F. Villinger, S. I. Staprans, R. R. Amara, J. M. Smith, J. G. Herndon, and H. L. Robinson. 2002. Slowly declining levels of viral RNA and DNA in DNA/recombinant modified vaccinia virus Ankara-vaccinated macaques with controlled simian-human immunodeficiency virus SHIV-89.6P challenge. *J. Virol.* 76: 10147–10154.
14. Radaelli, A., and C. De Giuli Morghen. 1994. Expression of HIV-1 envelope gene by recombinant avipox. *Vaccine* 12: 1101–1109.
15. Santra. S., J. E. Schmitz, M. J. Kuroda, M. A. Lifton, C. E. Nickerson, C. I. Lord, R. Pal, G. Franchini, and N. L. Letvin. 2002. Recombinant canarypox vaccine-elicited CTL specific for dominant and subdominant simian immunodeficiency virus epitopes in rhesus monkeys. *J. Immunol.* 168: 1847–1853.
16. Radaelli, A., C. Zanotto, G. Perletti, V. Elli, E. Vicenzi, G. Poli, and C. De Giuli Morghen. 2003. Comparative analysis of immune responses and cytokine profiles elicited in rabbits by the combined use of recombinant fowlpox viruses and virus-like particles in prime-boost vaccine protocols against SHIV. *Vaccine* 21: 2061–2073.
17. Hel, Z., J. Nacsa, W. P. Tsai, A. Thornton, L. Giuliani, J. Tartaglia, and G. Franchini. 2002. Equivalent immunogenicity of the highly attenuated poxvirus-based ALVAC-SIV and NYVAC-SIV vaccine candidate in SIVmac251-infected macaques. *Virology* 304: 125–134.
18. Hanke, T., R. V. Samuel, T. J. Blanchard, V. C. Neumann, T. M. Allen, J. E. Boyson, S. A. Sharpe, N. Cook, G. L. Smith, D. I. Watkins. et al. 1999. Effective induction of simian immunodeficiency virus-specific cytotoxic T lymphocytes in macaques by using a multiepitope gene and DNA prime-modified vaccinia virus Ankara boost vaccination regimen. *J. Virol.* 73: 7524–7532.
19. Mayr, A., H. Stickel, H. K. Muller, K. Danner, and H. Singer. 1978. The smallpox vaccination strain MVA: marker, genetic, structure, experience gained with the parenteral vaccination and behavior in organisms with a debilitated defense mechanism. *Zentralbl. Bakteriol. Ser. B* 167: 375–390.
20. Hanke, T., A. J. McMichael, R. V. Samuel, L. A. Powell, L. McLoughlin, S. J. Corme, and A. Edlin. 2002. Lack of toxicity and persistence in the mouse associated with administration of candidate DNA and modified vaccinia virus Ankara (MVA)-based HIV vaccine for Kenya. *Vaccine* 22: 108–114.
21. Ober, B. T., P. Bruhl, M. Schmidt, V. Wieser, W. Gritschenberger, S. Coulibaly, H. Savidis-Dacho, M. Gerencer, and F. G. Falkner. 2002. Immunogenicity and safety of defective vaccinia virus lister: comparison with modified vaccinia virus Ankara. *J. Virol.* 76: 7713–7723.
22. Ishii, K., Y. Ueda, K. Matsuo, Y. Matsuura, T. Kitamura, K. Kato, Y. Izumi, K. Someya, T. Ohsu, and M. Honda. 2002. Structure analysis of vaccinia virus DIs strain: application as a new replication-deficient viral vector. *Virology* 302: 433–444.
23. Someya, K., K. Q. Xin, K. Matsuo, K. Okuda, N. Yamamoto, and M. Honda. 2004. A consecutive prime-boost vaccination of mice with simian immunodeficiency virus (SHIV) gag/pol DNA and recombinant vaccinia virus strain DIs elicits anti-SIV immunity. *J. Virol.* 78: 9842–9853.
24. Tagaya, I., T. Kitamura, and Y. Sano. 1961. A new mutant of dermovaccinia virus. *Nature* 192: 381–382.
25. Tagaya, I., H. Amano, T. Kitamura, T. Komatsu, Y. Ueda, Y. Tanaka, N. Uchida, and H. Kodama. 1973. Properties of an attenuated mutant of vaccinia virus, strain DIs. *Symp. Ser. Immunobiol. Stand.* 19: 299–307.
26. Tagaya, I., H. Amano, T. Komatsu, N. Uchida, and H. Kodama. 1974. Supplement to the pathogenicity and immunogenicity of an attenuated vaccinia virus, strain DIs, in cynomolgus monkeys. *Jpn J. Med. Sci. Biol.* 27: 215–228.
27. Hutchings, C. L., S. C. Gilbert, A. V. S. Hill, and A. C. Moore. 2005. Novel protein and poxvirus-based vaccine combinations for simultaneous induction of humoral and cell-mediated immunity. *J. Immunol.* 175: 599–606.
28. Someya, K., D. Cecilia, T. Nakasone, Y. Ami, K. Matsuo, S. Burda, H. Yamamoto, N. Yoshino, M. Kaizu, S. Ando, et al. 2005. Vaccination of rhesus macaques with recombinant *Mycobacterium bovis* bacillus Calmette-Guérin (BCG)-Env V3 elicits neutralizing antibody-mediated protection against simian-human immunodeficiency virus with a homologous but not a heterologous V3 motif. *J. Virol.* 79: 1452–1462.
29. Sasaki, S., K. Sumino, K. Hamajima, J. Fukushima, N. Ishii, S. Kawamoto, H. Mohri, C. R. Kensil, and K. Okuda. 1998. Induction of systemic and mucosal immune responses to human immunodeficiency virus type 1 by a DNA vaccine formulated with QS-21 saponin adjuvant via intramuscular and intranasal routes. *J. Virol.* 72: 4931–4939.
30. Sasaki, Y., Y. Ami, T. Nakasone, K. Shinohara, E. Takahashi, S. Ando, K. Someya, Y. Suzaki, and M. Honda. 2002. Induction of CD95 ligand expression on T lymphocytes and B lymphocytes and its contribution to apoptosis of CD95-upregulated $CD4^+$ T lymphocytes in macaques by infection with a pathogenic simian/human immunodeficiency virus. *Clin. Exp. Immunol.* 122: 381–389.
31. Shinohara, K., K. Sakai, S. Ando, Y. Ami, N. Yoshino, E. Takahashi, K. Someya, Y. Suzaki, T. Nakasone, Y. Sasaki, et al. 1999. A highly pathogenic simian/human immunodeficiency virus with genetic changes in cynomolgus monkeys. *J. Gen. Virol.* 80: 1231–1240.
32. Yoshino, N., T. Ryu, M. Sugamata, T. Ihara, Y. Ami, K. Shinohara, F. Tashiro, and M. Honda. 2000. Direct detection of apoptotic cells in peripheral blood from highly pathogenic SHIV-inoculated monkeys. *Biochem. Biophys. Res. Commun.* 268: 868–874.
33. Lu, Y., M. S. Salvato, C. D. Pauza, J. Li, J. Sodroski, K. Manson, M. Wyand, N. Letvin, S. Jenkins, N. Touzjian, et al. 1996. Utility of SHIV for testing HIV-1 vaccine candidates in macaques. *J. Acquired Immune Defic. Syndr. Hum. Retrovirol.* 12: 99–106.
34. Reimann, K. A., J. T. Li, G. Voss, C. Lekutis, K. Tenner-Racz, P. Racz, W. Lin, D. C. Montefiori, D. E. Lee-Parritz, Y. Lu, et al. 1996. An *env* gene derived from a primary human immunodeficiency virus type 1 isolate confers high in vivo replicative capacity to a chimeric simian/human immunodeficiency virus in rhesus monkeys. *J. Virol.* 70: 3198–3206.
35. Mothe, B. R., H. Horton, D. K. Carter, T. M. Allen, M. E. Liebl, P. Skinner, T. U. Vogel, S. Fuenger, K. Vielhunber, W. Rehrauer, et al. 2002. Dominance of CD8 responses specific for epitopes bound by a single major histocompatibility complex class I molecule during the acute phase of viral infection. *J. Virol.* 76: 875–884.
36. Barouch, D. H., S. Santra, J. E. Schmitz, M. J. Kuroda, T. M. Fu, W. Wagner, M. Bilska, A. Craiu, X. X. Zheng, G. R. Krivulka, et al. 2000. Control of viremia and prevention of clinical AIDS in rhesus monkeys by cytokine-augmented DNA vaccination. *Science* 290: 486–492.

37. Carroll, M. W., and B. Moss. 1997. Host range and cytopathogenicity of the highly attenuated MVA strain of vaccinia virus: propagation and generation of recombinant viruses in a nonhuman mammalian cell line. *Virology* 238: 198–211.
38. Ober, B. T., O. Bruhl, M. Schmidt, V. Wieser, W. Gritschenberger, S. Coulibaly, H. Savidis-Dacho, M. Gerencer, and F. G. Falkner. 2002. Immunogenicity and safety of defective vaccinia virus lister: comparison with modified vaccinia virus Ankara. *J. Virol.* 76: 7713–7723.
39. Ami, Y., Y. Izumi, K. Matsuo, K. Someya, M. Kanekiyo, S. Horibata, N. Yoshino, K. Sakai, K. Shinohara, S. Yamazaki, et al. 2005. Prime-boost vaccination with recombinant *Mycobacterium bovis* bacillus Calmette Guérin and a non-replicating vaccinia virus recombinant leads to long-lasting and effective immunity. *J. Virol.* 79: 12871–12879.
40. Putkonen, P., M. Quesada-Rolander, A. C. Leandersson, S. Schwartz, R. Thorstensson, K. Okuda, B. Wahren, and L. Hinkula. 1998. Immune responses but no protection against SHIV by gene-gun delivery of HIV-1 DNA followed by recombinant subunit protein boosts. *Virology* 250: 293–301.
41. Vogel, T. U., M. R. Reynolds, D. H. Fuller, K. Vielhuber, T. Shipley, J. T. Fuller, K. J. Kunstman, G. Sutter, M. L. Marthas, V. Erfle, et al. 2003. Multispecific vaccine-induced mucosal cytotoxic T lymphocytes reduce acute-phase viral replication but fail in long-term control of simian immunodeficiency virus SIVmac239. *J. Virol.* 77: 13348–13360.
42. Baker, E. 1997. $CD8^+$ cell-derived anti-human immunodeficiency virus inhibitory factor. *J. Infect. Dis.* 179 (Suppl. 3): S485–S488.
43. Zhang, L., W. Yu, T. He, J. Yu, R. E. Caffrey, E. A. Dalmasso, S. Fu, T. Pham, J. Mei, J. J. Ho, et al. 2002. Contribution of human α-defensin 1, 2, and 3 to the anti-HIV-1 activity of CD8 antiviral factor. *Science* 298: 995–1000.
44. Musey, L. K., J. N. Krieger, J. P. Hughes, T. W. Schacker, L. Corey, and M. J. McElrath. 1999. Early and persistent human immunodeficiency virus type 1 (HIV-1)-specific T helper dysfunction in blood and lymph nodes following acute HIV-1 infection. *J. Infect. Dis.* 180: 278–284.
45. Rosenberg, E. S., J. M. Billingsley, A. M. Caliendo, S. L. Boswell, P. E. Sax, S. E. Kalams, and B. D. Walker. 1997. Vigorous HIV-1-specific $CD4^+$ T cell responses associated with control of viremia. *Science* 278: 1447–1450.
46. Wilson, J. D., N. Imami, A. Watkins, J. Gill, P. Hay, B. Gazzard, M. Westby, and F. M. Gotch. 2000. Loss of $CD4^+$ T cell proliferative ability but not loss of human immunodeficiency virus type 1 specific equates with progression to disease. *J. Infect. Dis.* 182: 792–798.
47. Matloubian, M., R. J. Conception, and R. Ahmed. 1994. $CD4^+$ T cells are required to sustain $CD8^+$ cytotoxic T-cell responses during chronic viral infection. *J. Virol.* 68: 8056–8063.
48. Walter, E. A., P. D. Greenberg, M. J. Gilbert, R. J. Finch, K. S. Watanabe, E. D. Thomas, and S. R. Riddell. 1995. Reconstitution of cellular immunity against cytomegalovirus in recipients of allogeneic bone marrow by transfer of T-cell clone from the donor. *N. Engl. J. Med.* 338: 1038–1044.
49. Estcourt, M. J., A. J. Ramsay, A. Brooks, S. A. Thomson, C. J. Medveckz, and I. A. Ramshaw. 2002. Prime-boost immunization generates a high frequency, high-avidity $CD8^+$ cytotoxic T lymphocyte population. *Int. Immunol.* 14: 31–37.
50. Edwards, B. H., A. Bansal, S. Sabbaj, J. Bakari, M. J. Mulligan, and P. A. Goepfert. 2002. Magnitude of functional $CD8^+$ T-cell responses to the gag protein of human immunodeficiency virus type 1 correlates inversely with viral load in plasma. *J. Virol.* 76: 2298–2305.
51. Hel, Z., J. Nacsa, E. Tryniszewska, W. P. Tsai, R. W. Parks, D. C. Montefiori, B. K. Felber, J. Tartaglia, G. N. Pavlakis, and G. Franchini. 2002. Containment of simian immunodeficiency virus infection in vaccinated macaques: correlation with the magnitude of virus-specific pre- and after challenge $CD4^+$ and $CD8^+$ T cell responses. *J. Immunol.* 169: 4478–4487.
52. Seth, A., I. Ourmanov, M. J. Kuroda, J. E. Schmitz, M. W. Caroll, L. S. Wyatt, B. Moss, M. A. Forman, V. M. Hirsch, and N. L. Letvin. 1998. Recombinant modified vaccinia virus Ankara-simian immunodeficiency virus gag pol elicits cytotoxic T lymphocytes in rhesus monkeys by a major histocompatibility complex class I/peptide tetramer. *Proc. Natl. Acad. Sci. USA* 95: 10112–10116.
53. Robinson, S., W. A. Charini, M. H. Newberg, M. J. Kuroda, C. I. Lord, and N. L. Letvin. 2001. A commonly recognized simian immunodeficiency virus Nef epitope presented to cytotoxic T lymphocytes of Indian-origin rhesus monkeys by the prevalent major histocompatibility complex class I allele Mamu-A*02. *J. Virol.* 75: 10179–10186.
54. Seaman, M. S., S. Santra, M. H. Newberg, V. Philippon, K. Manson, L. Xu, R. S. Gelman, D. Panicali, J. R. Mascola, G. J. Nabel, et al. 2005. Vaccine-elicited memory cytotoxic T lymphocytes contribute to Mamu-A*01-associated control of simian/human immunodeficiency virus 89.6P replication in rhesus monkeys. *J. Virol.* 79: 4580–4588.
55. Miller, M. D., H. Yamamoto, A. L. Hughes, D. I. Watkins, and N. L. Letvin. 1991. Definition of an epitope and MHC class I molecule recognized by gag-specific cytotoxic T lymphocytes in SIV mac-infected rhesus monkeys. *J. Immunol.* 147: 320–329.
56. Yamamoto, H., M. D. Miller, H. Tubota, D. I. Watkins, G. P. Mazzara, V. Stallard, D. L. Panicali, A. Aldovini, R. A. Young, and N. L. Letvin. 1990. Studies of cloned simian immunodeficiency virus-specific T lymphocytes: gag-specific cytotoxic T lymphocytes exhibit a restricted epitope specificity. *J. Immunol.* 144: 3385–3389.
57. Morita, M., Y. Aoyama, M. Arita, H. Amona, H. Yoshizawa, S. Hashizume, T. Komatsu, and I. Tagaya. 1977. Comparative studies of several vaccinia virus strains by intrathalamic inoculation into cynomolgus monkeys. *Arch. Virol.* 53: 197–208.
58. Allen, T. M., P. Jing, P., B. Calore, H. Horton, D. H. O'Connor, T. Hanke, M. Piekarczyk, R. Ruddersdorf, B. R. Mothe, C. Emerson, et al. 2002. Effects of cytotoxic T lymphocytes (CTL) directed against a single simian immunodeficiency virus (SIV) Gag CTL epitope on the course of SIVmac239 infection. *J. Virol.* 76: 10507–10511.
59. Horton, H., T. U. Vogel, D. K. Carter, K. Vielhuber, D. H. Fuller, T. Shipley, J. T. Fuller, K. J. Kunstman, G. Sutter, D. C. Montefiori, et al. 2002. Effects of cytotoxic T lymphocytes (CTL) directed against a single simian immunodeficiency virus (SIV) Gag CTL epitope on the course of SIVmac239 infection. *J. Virol.* 76: 7187–7202.
60. Gruters, R. A., F. G. Terpstra, R. E. De Goede, J. W. Mulder, F. De Wolf, P. T. Schellekens, R. A. Van Lier, M. Tersmette, and F. Miedema. 1991. Immunological and virological markers in individuals progressing from seroconversion to AIDS. *AIDS* 5: 837–844.
61. Gruters, R. A., F. G. Terpstra, R. De Jong, C. J. Van Noesel, R. A. Van Lier, and F. Miedema. 1990. Selective loss of T cell function in different stages of HIV infection: early loss of anti-CD3-induced T cell proliferation followed by decreased anti-CD3-induced cytotoxic T lymphocyte generation in AIDS-related complex and AIDS. *Eur. J. Immunol.* 20: 1039–1044.
62. Jaleco, A. C., M. J. Covas, L. A. Pinto, and R. M. Victorino. 1994. Distinct alterations in the distribution of $CD45RO^+$ T-cell subsets in HIV-2 compared with HIV-1 infection. *AIDS* 8: 1663–1666.
63. Schnittman, S. M., H. C. Lane, J. Greenhouse, J. S. Justement, M. Baseler, and A. S. Fauci. 1990. Preferential infection of $CD4^+$ memory T cells by human immunodeficiency virus type 1: evidence for a role in the selective T-cell functional defects in infected individuals. *Proc. Natl. Acad. Sci. USA* 87: 6058–6062.
64. Van Noesel, C. J., R. A. Gruters, F. G. Terpstra, P. T. Schellekens, R. A. Van Lier, and F. Miedema. 1990. Functional and phenotypic evidence for a selective loss of memory T cells in asymptomatic human immunodeficiency virus-infected men. *J. Clin. Invest.* 86: 293–299.
65. Ginaldi, L., M. De Martinis, A. D'Ostilio, A. Di Gennaro, L. Marini, V. Profeta, and D. Quaglino. 1997. Activated naive and memory $CD4^+$ and $CD8^+$ subsets in different stages of HIV infection. *Pathobiology* 65: 91–99.
66. Miedema, F. 1992. Immunological abnormalities in the history of HIV infection: mechanisms and clinical relevance. *Immunodefic. Rev.* 3: 173–193.
67. Ullum, H., A. C. Lepri, J. Victor, P. Skinhoj, A. N. Phillips, and B. K. Pedersen. 1997. Increased losses of $CD4^+CD45RA^+$ cells in late stages of HIV infection is related to increased risk of death: evidence from a cohort of 347 HIV-infected individuals. *AIDS* 11: 1479–1485.
68. Choi, B. S., Y. K. Park, and J. S. Lee. 2002. The CD28/HLA-DR expression on $CD4^+$ T but not $CD8^+$ T cells are significant predictor for progression to AIDS. *Clin. Exp. Immunol.* 127: 137–144.
69. Kammerer, R., A. Iten, P. C. Feri, and P. Burgisser. 1996. Expansion of T cells negative for CD28 expression in HIV infection: relation to activation markers and cell adhesion molecules, and correlation with prognostic markers. *Med. Microbiol. Immunol.* 185: 19–25.

Efficient intervention of growth and infiltration of primary adult T-cell leukemia cells by an HIV protease inhibitor, ritonavir

M. Zahidunnabi Dewan, Jun-nosuke Uchihara, Kazuo Terashima, Mitsuo Honda, Tetsutaro Sata, Mamoru Ito, Nobutaka Fujii, Kimiharu Uozumi, Kunihiro Tsukasaki, Masao Tomonaga, Yoko Kubuki, Akihiko Okayama, Masakazu Toi, Naoki Mori, and Naoki Yamamoto

Adult T-cell leukemia (ATL), an aggressive malignancy of CD4$^+$ T cells associated with human T-cell leukemia virus type I (HTLV-I) infection, carries a very poor prognosis because of the resistance of leukemic cells to any conventional regimen, including chemotherapy. We examined the effect of ritonavir, an HIV protease inhibitor, on HTLV-I–infected T-cell lines and primary ATL cells and found that it induced apoptosis and inhibited transcriptional activation of NF-κB in these cells. Furthermore, ritonavir inhibited expression of Bcl-x_L, survivin, c-Myc, and cyclin D2, the targets of NF-κB. In nonobese diabetic/severe combined immunodeficient (NOD/SCID)/γc^{null} (NOG) mice, ritonavir very efficiently prevented tumor growth and leukemic infiltration in various organs of NOG mice at the same dose used for treatment of patients with AIDS. Our data indicate that ritonavir has potent anti–NF-κB and antitumor effects and might be clinically applicable for treatment of ATL. These results would provide a new concept and novel platform for new drug development of leukemia and solid cancer as well. (Blood. 2006;107:716-724)

Introduction

Human T-cell leukemia virus type I (HTLV-I) is the causative agent of an aggressive form of CD4$^+$ T-cell leukemia designated adult T-cell leukemia (ATL).[1-3] ATL was first identified in Japan in 1977.[4,5] Common findings for patients with ATL include enlargement of peripheral lymph nodes, hepatomegaly, splenomegaly, hypercalcemia, and skin lesions. At present, there is no accepted curative therapy for ATL, and patients progress to death with a median survival duration of 13 months in aggressive ATL.[6] ATL has a poor prognosis mainly because of its resistance to conventional as well as high-dose chemotherapy.

ATL develops after a long period of latent infection. This long latency suggests that multiple genetic events, which accumulate in HTLV-I–infected cells, are involved in the development of ATL. However, the precise molecular mechanism of leukemogenesis and the development of ATL after HTLV-I infection are not fully elucidated. A unique viral gene *Tax* is considered to play a central role in HTLV-I–induced transformation, which is responsible for transactivation of the HTLV-I long terminal repeat,[7,8] as well as numerous cellular genes involved in T-cell activation and growth, such as those encoding IL-2,[9] and the α-chain of IL-2 receptor (IL-2Rα) (CD25, Tac).[10,11] Induction of many cellular genes by Tax is mediated through the transcription factor NF-κB. The malignant cells associated with all phases of ATL express very high levels of IL-2Rα[12-14] without expressing a significant amount of Tax.

HTLV-I–infected cell lines derived from a leukemic cell clone and primary ATL cells failed to express significant amounts of Tax and other viral proteins, suggesting that the expression of viral proteins is not always necessary for leukemic proliferation at the late stage of the disease. However, HTLV-I–infected cell lines and leukemic cells from patients with ATL display constitutive NF-κB binding activity and increased degradation of a specific inhibitor, IκBα.[15] In resting cells, NF-κB is sequestered as an inactive precursor by association with inhibitory IκBs in the cytoplasm. On stimulation, IκBs are rapidly phosphorylated, ubiquitinated, and degraded by a proteasome-dependent pathway, allowing active NF-κB to translocate into the nucleus where it can activate the expression of a number of genes.[16] NF-κB activation has been connected with multiple processes of oncogenesis, including control of apoptosis, cell cycle, differentiation, and cell migration[16]; therefore, inhibition of NF-κB was suggested to be a useful

From the Department of Molecular Virology, Graduate School of Medicine, Tokyo Medical and Dental University, Tokyo, Japan; the AIDS Research Center, National Institute of Infectious Diseases, Tokyo, Japan; the Division of Molecular Virology and Oncology, Graduate School of Medicine, University of the Ryukyus, Okinawa, Japan; the Department of Pathology, National Institute of Infectious Diseases, Tokyo, Japan; the Central Institute for Experimental Animals, Kanagawa, Japan; the Department of Bioorganic Medical Chemistry, Graduate School of Pharmaceutical Sciences, Kyoto University, Kyoto, Japan; the Department of Epidemiology and Preventive Medicine, Kagoshima University Graduate School of Medical and Dental Sciences, Kagoshima, Japan; the Department of Hematology, Molecular Medicine Unit, Atomic Bomb Disease Institute, Nagasaki University Graduate School of Biomedical Sciences, Nagasaki, Japan; the Second Department of Internal Medicine, Miyazaki Medical College, University of Miyazaki, Miyazaki, Japan; the Department of Laboratory Medicine, Miyazaki Medical College, University of Miyazaki, Miyazaki, Japan; and the Division of Clinical Trials and Research, Breast Cancer Research and Treatment Program, Tokyo Metropolitan Komagome Hospital, Tokyo Medical Center for Cancer and Infectious Disease, Tokyo, Japan.

Submitted February 23, 2005; accepted September 1, 2005. Prepublished online as *Blood* First Edition Paper, September 20, 2005; DOI 10.1182/blood-2005-02-0735.

Supported by grants from the Ministry of Education, Science, and Culture; the Ministry of Health, Labor, and Welfare; and Human Health Science of Japan.

M.Z.D. and J.U. contributed equally to the study.

Reprints: Naoki Yamamoto, Department of Molecular Virology, Graduate School of Medicine, Tokyo Medical and Dental University, 1-5-45 Yushima, Bunkyo-ku, Tokyo 113-8519, Japan; e-mail: *yamamoto.mmb@tmd.ac.jp*; and Naoki Mori, Division of Molecular Virology and Oncology, Graduate School of Medicine, University of the Ryukyus, 207 Uehara, Nishihara, Okinawa 903-0215, Japan; e-mail: n-mori@med.u-ryukyu.ac.jp.

The publication costs of this article were defrayed in part by page charge payment. Therefore, and solely to indicate this fact, this article is hereby marked "advertisement" in accordance with 18 U.S.C. section 1734.

strategy for cancer therapy.[17-20] Despite the diversity in clinical manifestations of ATL, strong and constitutive NF-κB activation was reported to be a unique and common characteristic of ATL cells.[15] Thus, the indispensability of NF-κB for the maintenance of the malignant phenotype of HTLV-I provides a possible molecular target for ATL therapy.[21-24]

Ritonavir, a human immunodeficiency virus type 1 (HIV-1) protease inhibitor (PI), has been successfully used in clinical treatments of HIV infection, with patients exhibiting a marked decrease in HIV viral load and a subsequent increase in $CD4^+$ T-cell counts.[25-28] Evidence of other effects by ritonavir on cellular proteases, such as the cysteine proteases cathepsin D and E, was presented in the drug's original description, albeit at concentrations greater than 500-fold above the concentration required for inhibition of HIV protease.[29] PIs have also been shown to directly affect cell metabolism, interfere with host or fungal proteases, and block T-cell activation and dendritic cell function.[30,31] Recently, ritonavir has been shown to inhibit the chymotrypsin-like activity of the 20S proteasome, and it activates the chymotrypsin-like activity of the 26S proteasome conversely.[30,32,33] Ritonavir also has been reported to inhibit the transactivation of NF-κB induced by activators such as TNFα, HIV-1 Tat protein, and the human herpesvirus 8 protein ORF74. It is possible that inhibition of NF-κB activation by ritonavir is linked to additional pathways other than inhibition of proteasome.[34] PIs also have been shown to have direct antiangiogenic and antitumor activity[34,35]

In this study, we investigated the antitumor effects of ritonavir on HTLV-I–infected cell lines and primary ATL cells. We found that ritonavir decreases NF-κB activity linked to the inhibition of IκBα phosphorylation and induces apoptosis of these cells. In addition, we established preclinical models to evaluate the efficacy of anti-ATL and anti–NF-κB therapies. In the ATL model, ritonavir potently inhibited the growth and infiltration of leukemic cells from patients at concentrations used for treatment of patients with AIDS.

Materials and methods

Cell lines

The T-cell leukemia cell line Jurkat, HTLV-I–infected T-cell lines MT-2,[36] MT-4,[37] C5/MJ,[38] SLB-1,[39] HUT-102,[2] MT-1,[40] and ED-40515(−),[41] and bcr-abl$^+$ leukemic cell line K562 were cultured in RPMI 1640 medium supplemented with 2% heat-inactivated fetal bovine serum (JRH Biosciences, Lenexa, KS), 100 U/mL penicillin, and 10 μg/mL streptomycin. MT-2, MT-4, C5/MJ, and SLB-1 are HTLV-I–transformed T-cell lines. MT-1 and ED-40515(−) are T-cell lines of leukemic cell origin established from patients with ATL. The clonal origin of HUT-102 is unclear.

Human specimens

Leukemic cells from 38 patients (8 patient samples for in vitro studies, 20 for establishment of ATL model, 10 for in vivo ritonavir studies) diagnosed as either acute type or chronic type were used in this study. The diagnosis of ATL was based on clinical features, hematologic findings, and the presence of anti–HTLV-I antibodies in the sera. Baseline characteristics for the patients who entered the study are shown in Table 1. Monoclonal HTLV-I provirus integration into the DNA of leukemia cells was confirmed by Southern blot hybridization in all cases (data not shown). All samples were collected after obtaining informed consent from patients. Peripheral blood mononuclear cells (PBMCs) from healthy volunteers and patients with ATL were purified by Ficoll-Hypaque gradient centrifugation (Amersham Biosciences, Uppsala, Sweden) and washed with RPMI 1640.

Growth inhibition assay

The effect of ritonavir on cell growth was assayed by the WST-8 method as described previously.[42] The WST-8 Cell Counting Kit was obtained from Wako Chemicals (Osaka, Japan). Briefly, 2×10^5 cells were incubated in a 96-well microculture plate in the absence or presence of various concentrations of ritonavir. After 72 hours of culture, 10 μL WST-8 solution was added, and the cells were incubated for another 2 hours. The number of surviving cells was measured with a microplate reader at a reference wavelength of 655 nm and test wavelength of 450 nm. Cell viability was determined as the percentage of the control (ie, absence of ritonavir).

Assay for apoptosis

Quantification of apoptosis was performed by immunostaining cells with Apo2.7, which specifically detects the 38-kDa mitochondrial membrane antigen 7A6 present only on the mitochondrial membrane of apoptotic cells, and so can be used as an early apoptotic marker in cells.[43,44] Cells cultured for 72 hours in the absence or presence of various concentrations of ritonavir were labeled with the Apo2.7-phycoerythrin–conjugated monoclonal antibody (Beckman-Coulter/Immunotech, Miami, Florida) or mouse IgG1 isotype control (Beckman-Coulter/Immunotech) and subsequently analyzed by flow cytometry.

EMSA

Cells were placed in culture at 1×10^6 cells/mL (cell line) or 5×10^6 cells/mL (PBMCs) and examined for inhibition of NF-κB after exposure to ritonavir. Nuclear proteins were extracted, and NF-κB binding activities to κB element were examined by electrophoretic mobility shift assay (EMSA) as described previously.[15] In brief, 5 μg nuclear extracts were preincubated in a binding buffer containing 1 μg poly(dI:dC) (Amersham Biosciences), followed by addition of ^{32}P-labeled oligonucleotide probe containing NF-κB element (5×10^4 cpm). These mixtures were incubated for 15 minutes at room temperature. The DNA-protein complexes were separated on a 4% polyacrylamide gel and visualized by autoradiography. To examine the specificity of the NF-κB element probe, unlabeled competitor oligonucleotides were preincubated with nuclear extracts for 15 minutes before incubation with probes. The probe or competitors used were prepared by annealing the sense and antisense synthetic oligonucleotides as follows: a typical NF-κB element from the *IL2RA* gene, 5′-gatcCGGCAGGGGAATCTCCCTCTC-3′; and AP-1 element of the *IL8* gene, 5′-gatcGTGATGACTCAGGTT-3′. Underlined sequences represent the NF-κB or AP-1 binding site. To identify NF-κB proteins in the DNA protein complex revealed by EMSA, we used antibodies specific for various NF-κB proteins, including p65, p50, c-Rel, and p52 (Santa Cruz Biotechnology, Santa Cruz, CA), to elicit a supershift DNA protein complex formation. These antibodies were incubated with the nuclear extracts for 45 minutes at room temperature before incubation with radiolabeled probes.

Western blot analysis

Treated cells were solubilized at 4°C in lysis buffer containing 62.5 mM Tris-HCl (pH 6.8), 2% SDS, 10% glycerol, 6% 2-mercaptoethanol, and 0.01% bromophenol blue. Samples were subjected to electrophoresis on SDS-polyacrylamide gels followed by transfer to a polyvinylidene difluoride membrane and probing with the following specific antibodies: polyclonal antibodies against IκBα, cIAP2, survivin, cyclin D2 (Santa Cruz Biotechnology), Bcl-X_L (Transduction Laboratories, San Jose, CA), and c-Myc (NeoMarkers, Fremont, CA) and monoclonal antibodies against phospho-IκBα, hyperphosphorylated form of pRb (Cell Signaling Technology, Beverly, MA), Bcl-2, and actin (NeoMarkers). The protein bands recognized by the antibodies were visualized using the enhanced chemiluminescence system (Amersham, Piscataway, NJ).

Plasmids and transfection

Reporter plasmid κB-LUC (kindly provided by J. Fujisawa, Kansai Medical University, Osaka, Japan) is a luciferase expression plasmid controlled by 5 tandem repeats of a NF-κB binding site from the *IL2RA*

Table 1. Clinical characteristics of patients

Patient	Age, y/sex	Diagnosis	WBC count, cells × 10^9/L	Lymphocytes, %	Atypical cells, %	Treatment status
1	54/M	Acute	192.80	65.0	91.0	Untreated
2	77/F	Acute	186.0	41.0	70.0	Untreated
3	67/F	Chronic	10.40	38.0	89.0	Treated
4	58/M	Acute	67.30	71.0	80.0	Treated
5	71/M	Acute	19.70	51.0	61.0	Treated
6	66/F	Chronic	29.40	49.0	75.0	Untreated
7	48/F	Chronic	9.40	29.0	55.0	Untreated
8	69/F	Acute	53.80	44.0	95.0	Treated
9	58/M	Chronic	11.30	59.0	70.0	Treated
10	60/M	Chronic	9.12	61.0	80.0	Treated
11	65/F	Acute	29.40	25.0	60.0	Untreated
12	49/F	Chronic	15.10	48.0	75.0	Treated
13	57/M	Chronic	10.00	50.0	57.0	Treated
14	72/F	Acute	39.00	70.0	80.0	Treated
15	79/F	Chronic	10.10	47.0	27.0	Untreated
16	68/F	Acute	7.00	86.0	86.0	Treated
17	59/F	Chronic	8.99	74.5	40.0	Treated
18	70/M	Acute	31.60	71.7	68.0	Treated
19	49/M	Acute	5.00	19.5	78.0	Treated
20	44/M	Chronic	36.40	33.0	43.0	Untreated
21	65/F	Chronic	14.70	76.0	22.0	Untreated
22	63/F	Acute	12.40	71.0	82.0	Untreated
23	56/F	Chronic	7.20	46.0	15.0	Treated
24	78/F	Acute	94.50	63.3	49.0	Treated
25	62/F	Acute	10.10	53.0	27.0	Untreated
26	66/M	Chronic	38.10	63.0	39.0	Treated
26	39/F	Chronic	18.50	16.0	57.0	Untreated
28	48/F	Acute	53.50	39.0	64.0	Untreated
29	75/F	Acute	15.00	72.0	65.0	Untreated
30	84/F	Acute	14.40	69.0	61.0	Treated
31	73/M	Chronic	7.80	59.0	47.0	Untreated
32	43/F	Chronic	18.60	63.0	43.0	Untreated
33	54/F	Acute	69.00	49.0	50.0	Untreated
34	66/F	Acute	10.20	38.0	51.0	Untreated
35	73/F	Chronic	15.70	58.0	39.0	Untreated
36	63/F	Acute	32.90	71.0	95.0	Treated
37	44/F	Chronic	22.60	51.0	45.0	Untreated
38	68/M	Acute	30.00	79.0	81.0	Untreated

WBC indicates white blood cells.

gene. Reporter plasmid AP-1–LUC (kindly provided by N. Mukaida, Kanazawa University, Kanazawa, Japan) is a luciferase expression plasmid controlled by 2 copies of the AP-1 binding site from the IL-8 promoter. The expression plasmid for HTLV-I Tax has been described previously.[45] Transient transfections were performed in Jurkat and HUT-102 cells by electroporation using 5×10^6 cells and reporter and effecter plasmids. To normalize transfection efficiencies, a thymidine kinase (TK) promoter-driven *Renilla* luciferase plasmid (phRL-TK; Promega, Madison, WI) was cotransfected as an internal control plasmid. Then, 16 hours after transfection, ritonavir was added to the cultures at various concentrations, and cells were further cultured for 24 hours for assay of luciferase activity. Transfected cells were collected by centrifugation, washed with phosphate-buffer saline (PBS), and lysed in reporter lysis buffer (Promega). Lysates were assayed for reporter gene activity with the dual-luciferase reporter assay system (Promega).

Inoculation of ATL cells and collection of samples

NOG mice were obtained from the Central Institute for Experimental Animals (Kawasaki, Japan). All mice were maintained under specific pathogen-free conditions in the Animal Center of National Institute of Infectious Diseases (Tokyo, Japan). The Ethical Review Committee of the Institute approved the experimental protocol. Mice were anesthetized with ether, and cells were inoculated either intraperitoneally in abdominal region or subcutaneously in the postauricular region of NOG mice without injection of human recombinant IL-2 at a dose of 1 to 2×10^7 cells per mouse. All mice were killed 30 or 60 days after inoculation with primary ATL cells. Blood was collected from the tail to make a smear, as well as from the heart with heparinized syringes. PBMCs and splenocytes were isolated by density gradient concentration with Ficoll-Hypaque. Blood smear slides were fixed in methyl alcohol for May-Grunwald and Giemsa staining. PBMCs and splenocytes were stored at −80°C for further experiments. Tissues and various organs of mice were collected and fixed with Streck Tissue Fixative, then processed to paraffin wax-embedded sections for staining with hematoxylin and eosin (HE) and immunostaining.

Treatment of ATL mice with ritonavir

Ritonavir was obtained from Abbott Labs, North Chicago, IL. Primary ATL cells (2×10^7) from 10 patients were inoculated subcutaneously in the postauricular region of NOG mice. One day after inoculation of ATL cells, mice were treated with either RPMI 1640 (control mice) or drug (ritonavir 30 mg/kg/d) intraperitoneally daily for 30 days followed by observation for another 30 days without treatment. ATL cell growth and progression were monitored by observation of physical condition of mice during a 2-month follow-up period.

Immunohistochemistry

Paraffinized cryosections of various organs were deparaffinized and hydrated in xylenes or clearing agents and graded alcohol series, then rinsed for 5 minutes in water. Deparaffinized samples were incubated with 0.025% trypsin/PBS for 30 minutes followed by washing, and then incubated with 0.3% methanol for 30 minutes at room temperature and washed 2 times with PBS. Immunostaining was done as described previously[46] using Vector MOM immunodetection kit (Vector Labs, Burlingame CA) for ATL cells with a 1:500 dilution of primary mouse monoclonal antibody specific for human CD4 and CD25 (Dako, Caterpillar, CA). This was followed by washing in PBS and incubation with a secondary antibody MOM biotinylated anti–mouse IgG, after which cells were again washed in PBS and incubated with VECTASTAIN *Elite* ABC for 20 minutes at room temperature. Positive staining was visualized after incubation of these samples with a mixture of 0.05% 3,3′-diaminobenzidine tetrahydrochloride in 50 mM Tris-HCl buffer and 0.01% hydrogen peroxide for 5 minutes. The samples were counterstained with hematoxylin for 2 minutes, hydrated completely, cleaned in xylene, and then mounted. Photographs were taken by light microscopy (BX41, Olympus, Tokyo, Japan) using UplanF1 lenses (DP70, Olympus; magnification ×40).

Results

Ritonavir reduces cell growth and induces apoptosis of HTLV-I–infected cell lines and primary ATL cells

Ritonavir was examined for its effect on proliferation of HTLV-I–infected cell lines (Figure 1A). Ritonavir effectively inhibited the proliferation of HTLV-I–infected cell lines as measured by WST-8 on the third day of culture in a dose-dependent manner, but not that of K562 cells. Further experiments using Apo2.7 showed that ritonavir caused apoptosis of HTLV-I–infected cell lines in a dose-dependent manner, but not that of K562 cells (Figure 1B-C). In addition, we explored the anti-ATL effect of ritonavir on freshly isolated ATL cells from patients. In all ATL cases, ritonavir reduced the survival of ATL cells in a dose-dependent manner (Figure 1D). Ritonavir also caused apoptosis of ATL cells (Figure 1E). In contrast, ritonavir hardly affected the survival of peripheral blood mononuclear cells (PBMCs) from 3 healthy volunteers as measured by WST-8 (Figure 1D).

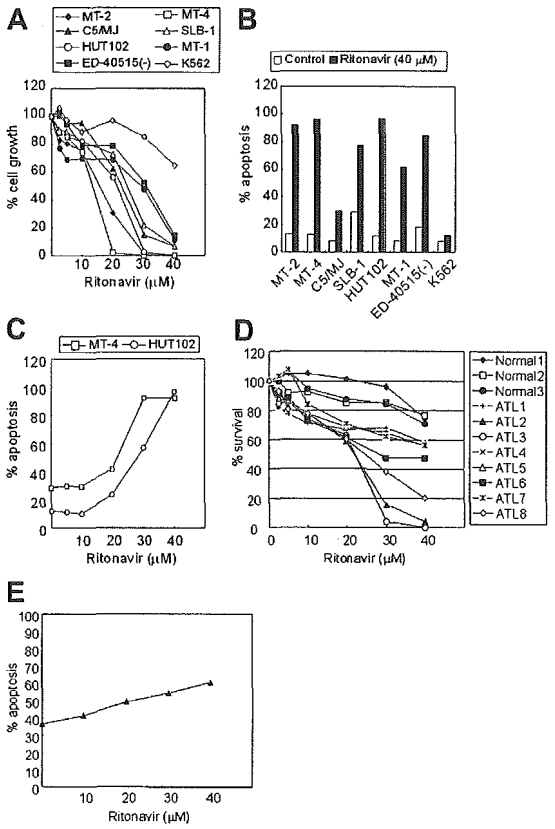

Figure 1. Effect of ritonavir on the growth and induction of apoptosis of HTLV-I–infected cell lines and freshly isolated ATL cells. (A) Dose-response effect of ritonavir on the growth of HTLV-I–infected cell lines. Cells (10^5/mL) were cultured for 72 hours in the presence of various concentrations (2.5-40 μM) of ritonavir. Cell growth was assessed by the water-soluble tetrazolium (WST)-8 method and is expressed as a percentage of control (untreated cells) and represents the mean of triplicate cultures. (B) Effect of ritonavir on induction of apoptosis of HTLV-I–infected cell lines. Cells were cultured for 72 hours with ritonavir (40 μM), and apoptosis was measured by Apo2.7 immunostaining. Data represent the mean percentages of apoptotic cells from both untreated (□) and ritonavir-treated (■) cells. (C) Dose-response effect of ritonavir on induction of apoptosis of MT-4 and HUT-102 cells. (D) Dose-response effect of ritonavir on the cell viability of freshly isolated ATL cells. Cells (10^6/mL) were cultured for 72 hours in the presence of various concentrations (2.5-40 μM) of ritonavir. (E) Dose-response effect of ritonavir on induction of apoptosis of ATL cells.

Ritonavir suppresses constitutive NF-κB expressed by HTLV-I–infected cell lines and primary ATL cells

To examine the effect of ritonavir on NF-κB DNA binding, electrophoretic mobility shift assay (EMSA) was performed. We first examined the minimum duration of exposure to ritonavir required for suppression of NF-κB. For this, HUT-102 cells were incubated with 40 μM ritonavir for different periods of time, and nuclear extracts were prepared and examined for NF-κB by EMSA. Down-regulation of NF-κB occurred at 24 hours in HUT-102 cells. However, no change in binding activity of AP-1 was observed (Figure 2A). The observed protein/DNA binding was specific for NF-κB, because the binding was effectively competed and abrogated by excess unlabeled NF-κB oligonucleotide but not by AP-1 (Figure 2C). The NF-κB complex contained p50, p65, and c-Rel (Figure 2C). Forty micromolar concentration of ritonavir was sufficient to suppress constitutive NF-κB activation in residual HTLV-I–infected T-cell lines (data not shown). It should be noted that K562 cells did not show constitutive NF-κB activation (data not shown). We also found a concentration-dependent inhibitory effect of ritonavir on the constitutive increase of NF-κB DNA binding activity (Figure 2B). Twenty micromolar concentration of ritonavir caused only a partial inhibition of NF-κB/DNA binding, whereas strong inhibition was observed at 30 and 40 μM in HUT-102 cells. However, AP-1 binding was not inhibited. This inhibition coincided with an accumulation of unphosphorylated IκBα and a decrease of the slower-migrating form of phosphorylated IκBα, a prerequisite for its subsequent degradation (Figure 2D, top). Thirty micromolar concentration of ritonavir caused only a partial decrease of the slower-migrating form of phosphorylated IκBα, whereas significant decrease of the slower-migrating form of phosphorylated IκBα and an accumulation of unphosphorylated IκBα were observed at 40 μM. We determined the alteration of phosphorylation of IκBα using antibody against phosphospecific IκBα. Results in Figure 2D (middle) show that 40 μM ritonavir decreased the phosphorylated IκBα content. We also determined whether the same results were obtained in primary ex vivo ATL specimens. As shown in Figure 2E, the amount of NF-κB that translocates to the nucleus is also decreased, as determined by EMSA. Twenty micromolar concentration of ritonavir caused only a partial inhibition of NF-κB/DNA binding, whereas strong inhibition was observed at 30 μM in primary ATL cells from acute

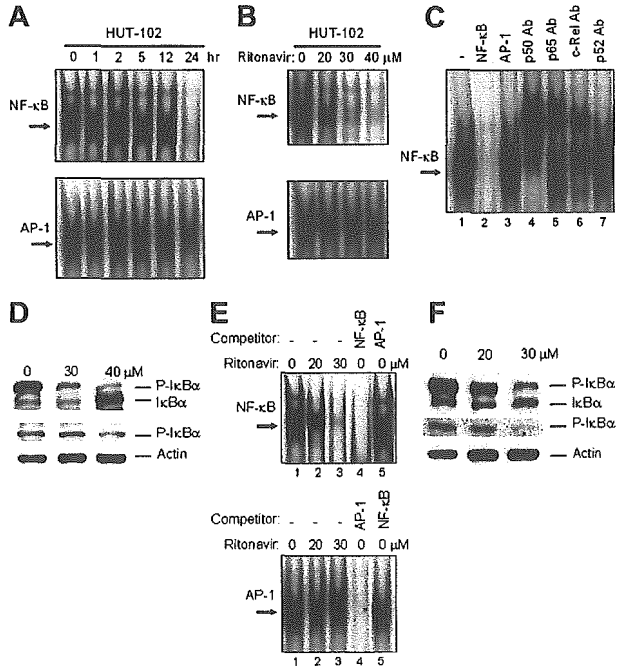

Figure 2. Ritonavir inhibits constitutive NF-κB activation. (A) HUT-102 cells treated with ritonavir (40 μM) for the indicated time were evaluated for NF-κB and AP-1 activation. (B) HUT-102 cells treated with the indicated concentration of ritonavir for 24 hours were evaluated for NF-κB and AP-1 activation. (C) Cold competition using 100-fold molar excess of unlabeled NF-κB and AP-1 oligonucleotides (lanes 2 and 3) demonstrated the specificity of the protein/DNA binding complexes. Specificity of NF-κB binding was also determined by using antibodies to the NF-κB components p50, p65, c-Rel, and p52, resulting in supershift (lanes 4-7). (D) HUT-102 cells were treated with the indicated concentration of ritonavir for 24 hours, and cell lysates were immunoblotted for IκBα (top) and phospho-IκBα (middle). Actin immunoblots confirm that similar amounts of cell extracts were analyzed (bottom). (E) Primary acute-type ATL cells treated with concentrations of ritonavir as indicated for 24 hours were evaluated for NF-κB and AP-1 activation. Where indicated, 100-fold excess amounts of competitor oligonucleotides were added to the reaction mixture (lanes 4 and 5). (F) The bands of phosphorylated IκBα were down-regulated by ritonavir treatment. Detection of actin expression was used as an internal control.

type. However, AP-1 binding was not inhibited. Ritonavir abolished proximal signaling events leading to IκBα phosphorylation (Figure 2F). Twenty micromolar concentration of ritonavir caused only a partial decrease of the slower-migrating form of phosphorylated IκBα, whereas significant decrease of the slower-migrating form of phosphorylated IκBα and an accumulation of unphosphorylated IκBα were observed at 30 μM (top). Thirty micromolar concentration of ritonavir abolished the phosphorylated IκBα content (middle). We obtained similar results using another acute-type ATL cells (data not shown).

Ritonavir represses Tax-induced and constitutive transcriptional activity of NF-κB

We examined whether ritonavir inhibits the transcriptional activity of NF-κB. First, we tested the effect of ritonavir on Tax-induced NF-κB transcriptional activity in Jurkat cells (HTLV-I–uninfected cell line) transfected with Tax expression plasmid. Ritonavir caused only a partial inhibition of proliferation in Jurkat cells cultured for 24 hours even at the highest dose. Tax-induced NF-κB transcriptional activation was suppressed by ritonavir in a dose-dependent manner (Figure 3A). Next, we determined the effect of ritonavir on constitutively activated NF-κB and AP-1 transcriptional activity in an HTLV-I–infected cell line HUT-102. Ritonavir inhibited the constitutively activated transcriptional activity of NF-κB in a dose-dependent manner, but not that of AP-1 (Figure 3B). Twenty micromolar concentration of ritonavir caused only a partial inhibition of NF-κB/DNA binding (Figure 2B), whereas strong inhibition of NF-κB transcriptional activity was observed at the concentration less than 20 μM. This discrepancy might derive from differences in sensitivity between these 2 assays. These results indicate that ritonavir inhibits both Tax-induced and constitutive NF-κB transcriptional activity.

Ritonavir down-regulates the expression of NF-κB–regulated gene products

The antiproliferative and proapoptotic effects of ritonavir were explored by examining the level of intracellular regulators of cell cycle and apoptosis after exposure to ritonavir (Figure 3C). Ritonavir down-regulated levels of Bcl-X_L, survivin, cIAP2, c-Myc, cyclin D2, regulated by NF-κB,[47-51] and the phosphorylated form of pRb in HUT-102 cells cultured with 40 μM ritonavir for 72 hours. Thirty micromolar concentration of ritonavir caused only a partial down-regulation of Bcl-X_L and the phosphorylated form of pRb, whereas significant down-regulation of survivin was observed in HUT-102 cells cultured for 72 hours, suggesting that NF-κB–regulated genes have the differential sensitivity to ritonavir. However, ritonavir did not modulate levels of Bcl-2 and Tax proteins in these cells (Figure 3C; data not shown). We also explored the effect of ritonavir on NF-κB–regulated gene products in ATL cells freshly isolated from an acute-type patient. As shown in Figure 3D, Bcl-X_L, survivin, cyclin D2, and c-Myc, but not Bcl-2, showed a decline. Thus, expression of NF-κB regulated genes, the induction of which are involved in antiapoptosis (Bcl-X_L, survivin, and cIAP2) and cell cycle (cyclin D2 and c-Myc), apparently had been down-regulated in the presence of ritonavir. We obtained a similar result using other acute-type ATL

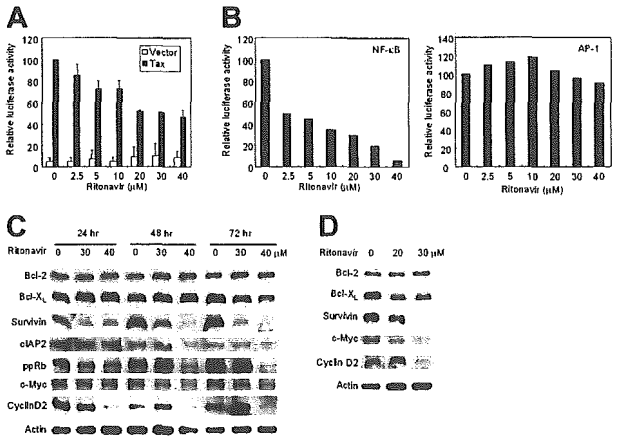

Figure 3. Ritonavir inhibits NF-κB transcriptional activation and expression of apoptosis- and cell-cycle–associated proteins. (A) Ritonavir inhibits Tax-induced NF-κB transcriptional activation. κB-LUC was transfected into Jurkat cells with Tax-expressing plasmid (■) or empty vector (□). After transfection, cells were treated with increasing concentrations of ritonavir. Luciferase activity is expressed relative to the basal level measured in cells transfected with the reporter plasmid and Tax-expressing plasmid without further treatment, which was defined as 100. Data represent the mean + SD from 3 independent experiments. (B) Ritonavir inhibits constitutive active NF-κB transcriptional activity in HUT-102 cells. κB-LUC and AP-1–LUC were transfected into HUT-102 cells. After transfection, cells were treated as in panel A. Luciferase activity was normalized, based on the Renilla luciferase activity from phRL-TK. Relative luciferase activity is expressed relative to the basal level measured in cells transfected with the reporter plasmid without further treatment, which was defined as 100. (C-D) Western blot analyses. HUT-102 cells (C) and primary acute-type ATL cells (D) were cultured with the indicated concentration of ritonavir for 24 to 72 hours (HUT-102 cells) and 24 hours (ATL cells). Cells were harvested and subjected to Western blot analysis. The polyvinylidene fluoride membrane was sequentially probed with indicated antibodies.

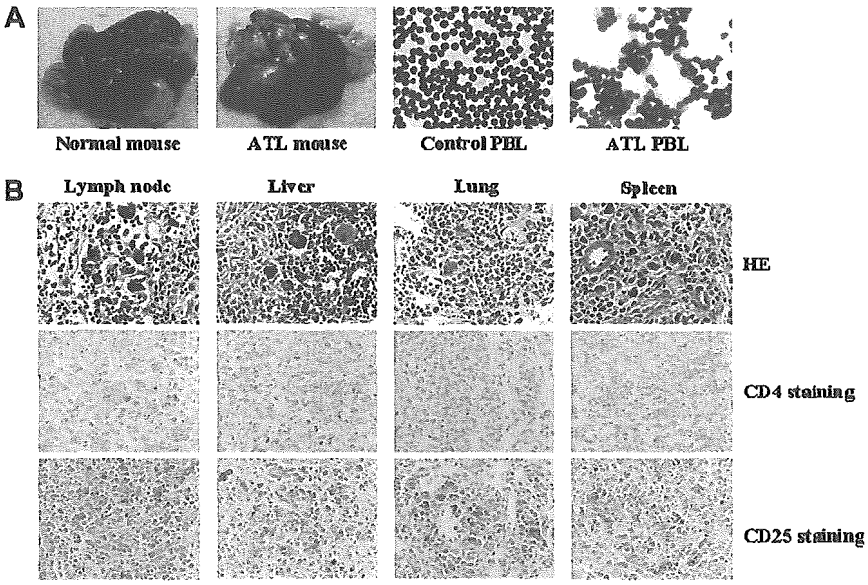

Figure 4. Successful engraftment and massive infiltration of primary ATL cells into various organs of NOG mice inoculated with PBMCs from patients with ATL. (A) Photographs of whole organs of normal and ATL cell–challenged mice with enlarged spleen, liver, and lungs (left 2 panels). Right 2 panels show May-Grunwald and Giemsa staining of PBMCs collected from normal and ATL cell–challenged mice, 2 months after inoculation of ATL cells, respectively. (B) HE (top) and immunohistochemical staining of various organs of NOG mice inoculated with ATL cells. Immunohistochemical staining using anti-CD4 (middle) and anti-CD25 (bottom) was conducted on various organs of mice tissues 2 months after inoculation of ATL cells. Magnification ×40.

cells (data not shown). Taken together these data suggest that constitutively high NF-κB activity in ATL cells is indispensable for their survival, and that specific inhibition of this activity by a clinically available drug results in the induction of apoptosis.

Establishment of a novel ATL model

PBMCs from patients with ATL were inoculated either intraperitoneally into the abdominal region or subcutaneously in the postauricular region of unconditional NOD/SCID/γc^{null} (NOG) mice. All mice developed clinical sign of near-death, such as piloerection, weight loss, and cachexia 6 to 8 weeks after inoculation of ATL cells in addition to the enlargement of lymph nodes, spleen, lungs, and liver, whereas no tumors were found in the postauricular region or abdominal cavity where primary ATL cells were inoculated (Figure 4A). There was no difference in respect to the successful engraftment of ATL cells inoculated either intraperitoneally or subcutaneously in NOG mice. Histologic analysis of ATL-bearing mice showed massive infiltration of leukemic cells in various organs of NOG mice that were efficiently expressing human CD4 and CD25 molecules (Figure 4B). A higher level of IL-2Rα (CD25) expression was observed on the surface of malignant cells associated with all stages of ATL[12-14] as well as ATL cells infiltrated into various organs of patients.[52,53] Thus, results from this model indicated successful engraftment and massive infiltration of primary ATL cells in various organs of NOG mice, like leukemia but without producing tumors at the sites of inoculation.

Ritonavir inhibits ATL cell growth and infiltration in NOG mice

To study the effect of ritonavir on ATL, we injected primary ATL cells (2×10^7) from 10 patients subcutaneously into the postauricular region of NOG mice. One day after inoculation, mice were treated with either RPMI-1640 (as control) or ritonavir (30 mg/kg/d) intraperitoneally daily for 30 days followed by observation for another 30 days without any treatment. ATL cell inoculation promoted the development of piloerection, weight loss, and cachexia, all of which are signs of near-death, in addition to the enlargement of lymph nodes, spleen, lungs, and liver in all control mice 2 months after inoculation (Figure 5A). In contrast, ritonavir-treated mice appeared to be healthy and had almost no enlargement of these organs (Figure 5A). Clinical evaluation of organ invasion 2 months after injection of primary ATL cells showed that ritonavir treatment inhibited their infiltration into lymph nodes, spleen, lungs, and liver (Figure 5B-D). Samples from 7 patients of 10 injected in mice treated with ritonavir presented substantial inhibition of organ invasion, and 2 (patients 5 and 7) showed partial inhibition, whereas one sample (patient 6) failed to do so (Table 2).

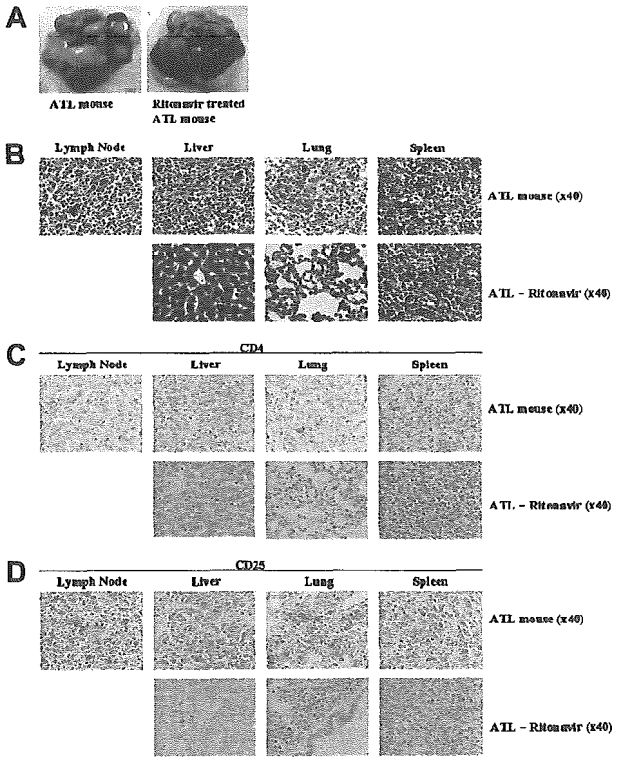

Figure 5. Effect of ritonavir on ATL cell growth and infiltration. (A) Mice were injected with ATL cells (2×10^7 cells) subcutaneously in the postauricular region. One day after inoculation, the mice were administered either RPMI 1640 or ritonavir (30 mg/kg/d) intraperitoneally every day for 30 days followed by observation for another month without therapy. Photographs of whole organs of RPMI 1640–treated ATL mice (left) and ritonavir-treated ATL mice (right) with enlarged spleen, liver, and lungs. (B-D) HE staining (B) and immunohistochemical staining using anti-CD4 (C) or anti-CD25 (D) in various organs of NOG mice 2 months after inoculation of ATL cells. Upper panels show various organs of mice treated with RPMI 1640, and lower panels represent various organs of mice treated with ritonavir. Magnification ×40.

Table 2. Effect of ritonavir on infiltration of ATL cells in various organs of SCID mice

Patient no. and treatment	Liver	Spleen	Lung	Lymph node
1				
Control	+++	+++	+++	+++
Ritonavir	++	+	+	NF
2				
Control	+++	+++	++	+++
Ritonavir	+	+	−	NF
3				
Control	+++	+++	+++	+++
Ritonavir	±	±	±	NF
4				
Control	+++	+++	+++	+++
Ritonavir	+	+	+	NF
5				
Control	+++	+++	+++	+++
Ritonavir	++	++	++	NF
6				
Control	+++	+++	+++	+++
Ritonavir	+++	++	+++	++
7				
Control	+++	+++	+++	+++
Ritonavir	++	+	++	NF
8				
Control	+++	+++	+++	+++
Ritonavir	±	±	±	NF
9				
Control	+++	+++	+++	++
Ritonavir	++	+	+	NF
10				
Control	+++	+++	++	+++
Ritonavir	+	+	+	NF

PBMCs from patients with ATL patients were inoculated subcutaneously into postauricular region of NOG mice, which were treated with ritonavir or RPMI-1640 as a control 1 day after inoculation for 1 month. Various organ infiltration was evaluated 2 months after inoculation.

NF indicates no formation of new lymph node; +++, massive; ++, marked; +, slight; ±, focally present or no infiltration; −, no infiltration.

In contrast, all control mice showed formation of new lymph nodes and infiltration with ATL cells into various organs (Figure 5B-D; Table 2). Organ infiltration of primary ATL cells was analyzed and evaluated by HE staining and immunostaining of CD4 and CD25. Together, these data indicate that ritonavir significantly inhibits ATL cell growth and infiltration in various organs of NOG mice (Figure 5).

Discussion

ATL is a malignancy of $CD4^+$ T-lymphocytes etiologically linked to a retrovirus, HTLV-I.[1-3] The malignant cells associated with all phases of ATL express very high levels of IL-2Rα (CD25).[12-14] The median survival duration of all patients with aggressive ATL was 13 months, and overall survival at 2 years was estimated to be 31.3%.[6] The various chemotherapies so far developed have not increased significantly the survival of patients with ATL. Given disappointing results using conventional chemotherapy, new approaches for the treatment of ATL are required. Previous reports have shown that primary ATL cells proliferate and infiltrate into various organs of SCID mice.[54-56] Our ATL model was consistent with others, but it represented more aggressive features about cell growth and infiltration in SCID mice. The tumor cells massively infiltrated into various organs in a manner similar to a leukemia-expressing T-cell marker CD4 and an activating marker CD25, especially into the spleen, lymph nodes, liver, and lungs of NOG mice. Our NOG ATL model presents many features 6 to 8 weeks after inoculation of ATL cells such as the clinical signs observed in patients with ATL. Two clinical types, acute and chronic, carry very different prognosis. However, no difference of cell growth, surface phenotype, and NF-κB activity is observed in primary leukemic cells from patients with acute- and chronic-type ATL. Therefore, the same characteristics of freshly isolated ATL cells with acute- and chronic-type were observed in NOG mice. Thus, it represents a novel model to evaluate tissue toxicity and the efficacy of therapeutic agents directed toward the treatment of ATL.

Constitutive NF-κB activation was demonstrated not only in HTLV-I–infected cell lines but also on fresh ATL cells regardless of Tax expression,[15] which could contribute to the drug-resistance of ATL cells through overexpression of Bcl-X_L.[51] We and others have previously reported that suppression of high NF-κB activity inhibited cell growth and induced apoptosis of HTLV-I–infected cell lines and primary ATL cells both in vitro and in vivo.[21-24] Recently, ritonavir has been shown to inhibit NF-κB activity induced by activators such as TNFα, Tat, and ORF74.[34] This led us to investigate whether this drug exhibits anti-ATL effects in vitro and in our preclinical murine ATL model. In the present study, we revealed that ritonavir treatment of HTLV-I–infected cell lines and ATL cells inhibited phosphorylation of IκBα, allowing suppression of NF-κB activity. Our results also suggest that inhibition of NF-κB activity by ritonavir reduced cell growth and induced apoptosis of these cells. This is consistent with down-modulation of NF-κB–regulated genes such as antiapoptotic (Bcl-X_L,[50,51] cIAP2,[57] and survivin[49]) and cell-cycle–related (cyclin D2[48] and c-Myc[47]) genes. We also examined the effect of ritonavir on the proliferation of an HTLV-I–negative T-cell line, Jurkat, in vitro. Exposure of ritonavir for 72 hours reduced the rate of proliferation (data not shown). Because ritonavir is suggested to affect proteasomal proteolysis,[33] it may effect a stabilization of p21, p27, and p53 proteins. Like proteasome inhibitors, ritonavir may also affect multiple pathways critical for survival of HTLV-I–positive and –negative malignant T cells. Additional experiments will be necessary to elucidate the mechanisms of anti-ATL activity.

In the therapy of HIV infection, the blood plasma ritonavir concentrations are between 5 and 15 μM,[58] but much higher maximal concentrations (up to 46 μM) have been determined in individual patients.[59] In the present study, we used the concentration of ritonavir for doing in vitro experiments from 0 to 40 μM and in vivo 30 mg/kg/d used for treatment of patients with AIDS. Our murine ATL model clearly indicates that 30 mg/kg/d of ritonavir significantly inhibits ATL cell growth and infiltration into various organs of NOG mice. The plasma exposure produced by this dose in mice is only approximately one half of the plasma exposure observed with the licensed dose of ritonavir in humans (600 mg twice daily). In our NOG ATL model, ritonavir at this treatment dosage is well tolerated without severe adverse effects observed in the mice during the treatment period. These data strongly suggest that the HIV PI, ritonavir, is a promising antitumor agent against ATL and could be used clinically for ATL regimens. Ritonavir exhibited anti-ATL activity against leukemic cells from patients

with acute- and chronic-type ATL in vitro and in vivo. The expression of CD25 and NF-κB activity do not differ between acute and chronic ATL cells.[12-15] These results suggest that anti-ATL activity of ritonavir correlates with suppression of NF-κB activity. It is also of interest to note that HTLV-I uses an aspartic protease analogous to HIV protease in its replication. To our knowledge, the activity of ritonavir against HTLV-I protease has not been assessed. Although Tax expression is very low or undetectable in ATL malignancy, a direct antiviral effect of ritonavir cannot be ruled out at this time.

In summary, using a large number of patient samples we have established a novel NOG ATL model that presents features similar to patients with ATL. These results also indicate that the HIV PI, ritonavir, showed antitumor and anti–NF-κB activity against primary ATL cells. Finally, our results strongly suggest that NF-κB serves as a potential molecular target to treat ATL, and that ritonavir might be used clinically as a single compound or in combination with the reducing dose of chemotherapeutic agents for treatment of patients with ATL.

Acknowledgments

We thank D. Kempf and T. Yamada of Abbott Laboratories, N. Yamamoto and S. Takeda of Molecular Virology, S. Ichinose of the Instrumental Analysis Research Center, S. Endo of the Animal Research Center, Tokyo Medical and Dental University, and P.J. Richard of Cardiff University for their advice and assistance with the experiments, and Y. Sato of the National Institute of Infectious Diseases for her excellent technical assistance. We thank J. Fujisawa for providing a luciferase reporter construct, κB-LUC, K. Matsumoto for providing the Tax expression plasmid, M. Maeda for providing ED-40 515(−), and the Fujisaki Cell Center, Hayashibara Biomedical Laboratories, for providing the MT-1, HUT-102, and C5/MJ cell lines.

References

1. Hinuma Y, Nagata K, Hanaoka M, et al. Adult T-cell leukemia: antigen in an ATL cell line and detection of antibodies to the antigen in human sera. Proc Natl Acad Sci U S A. 1981;78:6476-6480.
2. Poiesz BJ, Ruscetti FW, Gazdar AF, Bunn PA, Minna JD, Gallo RC. Detection and isolation of type C retrovirus particles from fresh and cultured lymphocytes of a patient with cutaneous T-cell lymphoma. Proc Natl Acad Sci U S A. 1980;77:7415-7419.
3. Yoshida M, Miyoshi I, Hinuma Y. Isolation and characterization of retrovirus from cell lines of human adult T-cell leukemia and its implication in the disease. Proc Natl Acad Sci U S A. 1982;79:2031-2035.
4. Takatsuki K, Uchiyama T, Sagawa K, Yodoi J. Adult T-cell leukemia in Japan. In: Seno S, Takaku F, Irino S, eds. Topics in Hematology. Amsterdam, The Netherlands: Excerpta Medica; 1977:73-77.
5. Uchiyama T, Yodoi J, Sagawa K, Takatsuki K, Uchino H. Adult T-cell leukemia: clinical and hematologic features of 16 cases. Blood. 1977;50:481-492.
6. Yamada Y, Tomonaga M, Fukuda H, et al. A new G-CSF-supported combination chemotherapy, LSG15, for adult T-cell leukaemia-lymphoma: Japan Clinical Oncology Group Study 9303. Br J Haematol. 2001;113:375-382.
7. Felber BK, Paskalis H, Kleinman-Ewing C, Wong-Staal F, Pavlakis GN. The pX protein of HTLV-I is a transcriptional activator of its long terminal repeats. Science. 1985;229:675-679.
8. Sodroski JG, Rosen CA, Haseltine WA. Trans-acting transcriptional activation of the long terminal repeat of human T lymphotropic viruses in infected cells. Science. 1984;225:381-385.
9. Maruyama M, Shibuya H, Harada H, et al. Evidence for aberrant activation of the interleukin-2 autocrine loop by HTLV-1-encoded p40x and T3/Ti complex triggering. Cell. 1987;48:343-350.
10. Ballard DW, Bohnlein E, Lowenthal JW, Wano Y, Franza BR, Greene WC. HTLV-I tax induces cellular proteins that activate the κB element in the IL-2 receptor α gene. Science. 1988;241:1652-1655.
11. Cross SL, Feinberg MB, Wolf JB, Holbrook NJ, Wong-Staal F, Leonard WJ Regulation of the human interleukin-2 receptor α chain promoter: activation of a nonfunctional promoter by the transactivator gene of HTLV-I. Cell. 1987;49:47-56.
12. Uchiyama T, Broder S, Waldmann TA. A monoclonal antibody (anti-Tac) reactive with activated and functionally mature human T cells, I: production of anti-Tac monoclonal antibody and distribution of Tac (+) cells. J Immunol. 1981;126:1393-1397.
13. Uchiyama T, Hori T, Tsudo M, et al. Interleukin-2 receptor (Tac antigen) expressed on adult T cell leukemia cells. J Clin Invest. 1985;76:446-453.
14. Waldmann TA, Greene WC, Sarin PS, et al. Functional and phenotypic comparison of human T cell leukemia/lymphoma virus positive adult T cell leukemia with human T cell leukemia/lymphoma virus negative Sezary leukemia, and their distinction using anti-Tac. Monoclonal antibody identifying the human receptor for T cell growth factor. J Clin Invest. 1984;73:1711-1718.
15. Mori N, Fujii M, Ikeda S, et al. Constitutive activation of NF-κB in primary adult T-cell leukemia cells. Blood. 1999;93:2360-2368.
16. Baldwin AS. The NF-κB and IκB proteins: new discoveries and insights. Annu Rev Immunol. 1999;14:649-681.
17. Watanabe M, Dewan MZ, Okamura T, et al. A novel NF-κB inhibitor DHMEQ selectively targets constitutive NF-κB activity and induces apoptosis of multiple myeloma cells in vitro and in vivo. Int J Cancer. 2005;114:32-38.
18. Adams J, Palombella VJ, Elliott PJ. Proteasome inhibition: a new strategy in cancer treatment. Invest New Drugs. 2000;18:109-121.
19. Teicher BA, Ara G, Herbst R, Palombella VJ, Adams J. The proteasome inhibitor PS-341 in cancer therapy. Clin Cancer Res. 1999;5:2638-2645.
20. Hideshima T, Chauhan D, Richardson P, et al. NF-κB as a therapeutic target in multiple myeloma. J Biol Chem. 2002;277:16639-16647.
21. Dewan MZ, Terashima K, Taruishi M, et al. Rapid tumor formation of human T-cell leukemia virus type 1-infected cell lines in novel NOD-SCID/γc^{null} mice: suppression by an inhibitor against NF-κB. J Virol. 2003;77:5286-5294.
22. Kitajima I, Shinohara T, Bilakovics J, Brown DA, Xu X, Nerenberg M. Ablation of transplanted HTLV-I Tax-transformed tumors in mice by antisense inhibition of NF-κB. Science. 1992;258:1792-1795.
23. Mori N, Yamada Y, Ikeda S, et al. Bay 11-7082 inhibits transcription factor NF-κB and induces apoptosis of HTLV-I–infected T-cell lines and primary adult T-cell leukemia cells. Blood. 2002;100:1828-1834.
24. Tan C, Waldmann TA. Proteasome inhibitor PS-341, a potential therapeutic agent for adult T-cell leukemia. Cancer Res. 2002;62:1083-1086.
25. Collier AC. Efficacy of combination antiretroviral therapy. Adv Exp Med Biol. 1996;394:355-372.
26. Collier AC, Coombs RW, Schoenfeld DA, Bassett R, Baruch A, Corey L. Combination therapy with zidovudine, didanosine and saquinavir. Antiviral Res. 1996;29:99.
27. Collier AC, Coombs RW, Schoenfeld DA, et al. Treatment of human immunodeficiency virus infection with saquinavir, zidovudine, and zalcitabine. AIDS Clinical Trials Group. N Engl J Med. 1996;334:1011-1017.
28. Markowitz M, Saag M, Powderly WG, et al. A preliminary study of ritonavir, an inhibitor of HIV-1 protease, to treat HIV-1 infection. N Engl J Med. 1995;333:1534-1539.
29. Kempf DJ, Marsh KC, Denissen JF, et al. ABT-538 is a potent inhibitor of human immunodeficiency virus protease and has high oral bioavailability in humans. Proc Natl Acad Sci U S A. 1995;92:2484-2488.
30. Andre P, Groettrup M, Klenerman P, et al. An inhibitor of HIV-1 protease modulates proteasome activity, antigen presentation, and T cell responses. Proc Natl Acad Sci U S A. 1998;95:13120-13124.
31. Liang JS, Distler O, Cooper DA, Jamil H, Deckelbaum RJ, Ginsberg HN, Sturley SL. HIV protease inhibitors protect apolipoprotein B from degradation by the proteasome: a potential mechanism for protease inhibitor-induced hyperlipidemia. Nat Med. 2001;7:1327-1331.
32. Schmidtke G, Holzhutter HG, Bogyo M, et al. How an inhibitor of the HIV-I protease modulates proteasome activity. J Biol Chem. 1999;274:35734-35740.
33. Gaedicke S, Firat-Geier E, Constantiniu O, et al. Antitumor effect of the human immunodeficiency virus protease inhibitor ritonavir: induction of tumor-cell apoptosis associated with perturbation of proteasomal proteolysis. Cancer Res. 2002;62:6901-6908.
34. Pati S, Pelser CB, Dufraine J, Bryant JL, Reitz MS Jr, Weichold FF. Antitumorigenic effects of HIV protease inhibitor ritonavir: inhibition of Kaposi sarcoma. Blood. 2002;99:3771-3779.
35. Sgadari C, Barillari G, Toschi E, et al. HIV protease inhibitors are potent anti-angiogenic molecules and promote regression of Kaposi sarcoma. Nat Med. 2002;8:225-232.
36. Miyoshi I, Kubonishi I, Yoshimoto S, et al. Type C virus particles in a cord T-cell line derived by cocultivating normal human cord leukocytes and